

# THERMALLY-ACTIVATED POST-GLITCH RESPONSE OF THE NEUTRON STAR INNER CRUST AND CORE. I: THEORY

Bennett Link

*Department of Physics, Montana State University, Bozeman, MT 59717, USA:*

`link@physics.montana.edu`

September 28, 2018

## ABSTRACT

Pinning of superfluid vortices is predicted to prevail throughout much of a neutron star. Based on the idea of Alpar et al., I develop a description of the coupling between the solid and liquid components of a neutron star through *thermally-activated vortex slippage*, and calculate the the response to a spin glitch. The treatment begins with a derivation of the vortex velocity from the vorticity equations of motion. The activation energy for vortex slippage is obtained from a detailed study of the mechanics and energetics of vortex motion. I show that the “linear creep” regime introduced by Alpar et al. and invoked in fits to post-glitch response is not realized for physically reasonable parameters, a conclusion that strongly constrains the physics of post-glitch response through thermal activation. Moreover, a regime of “superweak pinning”, crucial to the theory of Alpar et al. and its extensions, is probably precluded by thermal fluctuations. The theory given here has a robust conclusion that can be tested by observations: *for a glitch in spin rate of magnitude  $\Delta\nu$ , pinning introduces a delay in the post-glitch response time.* The delay time is  $t_d = 7(t_{sd}/10^4 \text{ yr})((\Delta\nu/\nu)/10^{-6})$  d where  $t_{sd}$  is the spin-down age;  $t_d$  is typically weeks for the Vela pulsar and months in older pulsars, and is independent of the details of vortex pinning. Post-glitch response through thermal activation cannot occur more quickly than this timescale. Quicker components of post-glitch response as have been observed in some pulsars, notably, the Vela pulsar, cannot be due to thermally-activated vortex motion but must represent a different process, such as drag on vortices in regions where there is no pinning. I also derive the mutual friction force for a pinned superfluid at finite temperature for use in other studies of neutron star hydrodynamics.

*Subject headings:* stars:neutron

## 1. Introduction

The problem of the origin of spin glitches in neutron stars has remained unsolved since the first glitch was observed in the Vela pulsar in 1969. This difficult problem is of considerable interest, as an understanding of the glitch phenomenon would offer insights into both the dynamical and ground-state properties of matter above nuclear density. To make progress on the glitch problem, it is crucial to identify which components of the liquid interior corotate with the crust, which store and release the angular momentum that drives glitches, and which produce the observed post-glitch response that occurs over days to years (for examples, see Lohsen 1975; Lyne 1987; Cordes et al. 1988; Shemar & Lyne 1996; Wang et al. 2000, 2001; Espinoza et al. 2011). A more complete understanding of the processes that regulate post-glitch response would be very useful for elucidating the dynamical properties of the neutron star interior. Fortunately, it is possible to address this problem without knowledge of the basic instability that causes glitches, and progress is possible with minimal assumptions.

The neutron star interior was predicted long ago to contain superfluid neutrons and superconducting protons (Migdal 1959; Ginzburg & Kirzhnits 1965; for recent reviews, see Dean & Hjorth-Jensen 2003 and Chamel & Haensel 2008). As in all rotating neutral superfluids, the neutron superfluid is threaded by an array of quantized vortices whose arrangement determines the angular momentum of the superfluid, and whose motion determines the torque exerted on the charged components of the star and the crust. In laboratory liquid helium, vortices *pin* to bumps on the bottom of the vessel, trapping the system in metastable rotational states. As the vessel is spun down, jumps in its spin rate are observed (Tsakadze & Tsakadze 1980), much like the glitches observed in neutron stars, as vortices unpin and the superfluid transfers angular momentum to the vessel.

Vortex pinning is predicted to occur throughout much of a neutron star, with the vortex lines pinning to sites along their length. In the inner crust, where a neutron superfluid coexists with the ionic lattice, vortices interact with nuclei with energies of  $\sim 1$  MeV per nucleus (Alpar 1977; Epstein & Baym 1988; Donati & Pizzochero 2006; Avogadro et al. 2007). This interaction pins the vortex lattice to the nuclear lattice, as confirmed by the simulations of Link (2009). In the outer core, the neutron flow around the vortices that thread the rotating superfluid entrains a proton mass current, strongly magnetizing the vortices as shown in the seminal work of Alpar et al. (1984c). Here the protons are expected to form a type II superconductor, with the magnetic flux arranged in flux tubes that are frozen to the highly-conductive charged component of the fluid. The proton superconductor rotates as a rigid body, without forming vortices. The vortices of the neutron superfluid pin to the flux tubes, primarily through a magnetic interaction, with pinning energies as high as

$\sim 100$  MeV per vortex-flux tube junction (Srinivasan et al. 1990; Jones 1991; Mendell 1991; Chau et al. 1992; Ruderman et al. 1998; Link 2012a). While pinning energies remain rather uncertain, the conclusion that vortices pin to inner-crust nuclei and outer-core flux tubes is on solid ground.

The nature of the glitch instability is a problem under active research, and many possibilities have been suggested. As originally suggested by Anderson & Itoh (1975), glitches could represent sudden unpinning of many vortices; as liberated vortices move under dissipation, a spin-up torque is exerted on the crust plus charged components. In this connection, glitches could arise through a vortex avalanche from a critical state (Cheng et al. 1988; Melatos et al. 2008). Other possibilities include increased frictional coupling from sudden heating of the crust (Greenstein 1979; Link & Epstein 1996) such as by a starquake, crust failure under superfluid stresses (Ruderman 1991), or interactions of magnetized flux tubes in the outer core with the London current near the core boundary (Sedrakian & Cordes 1999). Pizzochero (2011) has proposed that glitches result from the motion of a vortex sheet into a region where pinning is not sustainable. Alternatively, glitches might represent transitions between different states of superfluid turbulence (Peralta et al. 2006; Peralta & Melatos 2009; Glampedakis & Andersson 2009), though these studies do not account for vortex pinning which is likely to play an important role in the dynamics. Recent work has shown that pinning is hydrodynamically unstable in both the inner crust (Link 2012b) and the outer core (Link 2012a); further work is need to see how the instability saturates, and if the system turns turbulent.

Vortex pinning decreases the rotational coupling between the portions of the superfluid in which there is pinning and the rest of the star. If vortices remained perfectly pinned between glitches, the decoupling would be complete, and the superfluid would exert no torque on the charged components of the star (the crust, electrons, and core proton fluid). At finite temperature, though, vortices move through thermal activation over their pinning barriers, with an associated coupling time that is generally far longer than without pinning. Post-glitch response has been ascribed to internal torques exerted on the crust as the pinned superfluid responds to the glitch through thermally-activated vortex motion, as in the “vortex creep theory” of Alpar et al. (1984a), hereafter AAPS, that has been substantially developed and used to fit pulsar timing data (Alpar et al. 1984b, 1985, 1986, 1988, 1989, 1993, 1994, 1996).

In vortex creep theory there are two dynamical regimes: the “non-linear creep” regime introduced by AAPS, and the “linear creep” regime introduced by Alpar et al. (1989). In the “non-linear creep” regime, the system is always near the threshold for vortex unpinning. Post-glitch response is determined by two timescales, the *decoupling time*  $t_d$  and the

*recoupling time*  $t_r$ , and post-glitch response depends non-linearly on the size of the glitch.<sup>1</sup> Typical response in the “nonlinear” creep regime is depicted in Figure 8; the system remains out of equilibrium for a time  $t_d$ , before recovering over a time  $t_r$ , with a total response time of  $t_d + t_r$ . By contrast, in the “linear creep” regime post-glitch response depends linearly on the size of the glitch, and consists of simple exponential recovery over one timescale rather than two. The “linear creep” regime is generally associated with regions in which pinning is very weak, termed “superweak pinning” by AAPS.

The “non-linear creep regime” does admit linear response in the limit  $t_r \gg t_d$ . The important dynamical difference between the two regimes is that the total recovery time can be very short in the “linear creep” regime, but always exceeds  $t_d$  in the “non-linear” regime.

As vortex creep theory became more developed, terms were introduced in the crust response to account for internal torques from different parts of the star, vortex depletion regions, and crust cracking; see, *e.g.*, Alpar et al. (1996). Prompt exponential response is introduced by assuming the existence of regions that are in the “linear creep” regime. Fits to data introduce many free parameters, and do not offer conclusions with which the theory can be refuted. In particular, the “linear creep” regime, which gives simple exponential response independent of glitch magnitude, is not well-constrained by observations as it is observationally indistinguishable from vortex motion in a drag regime in which there is no pinning at all (see Section 3).

Inspired by the work of AAPS, the purpose of this paper is to present a comprehensive theory of thermally-activated vortex motion in the inner crust and the outer core with which to interpret existing and future glitch data and, in particular, to make *falsifiable predictions*. The theory developed here, which I call “thermally-activated vortex slippage” or “vortex slippage”, to distinguish it from the “vortex creep theory” of AAPS, begins with a derivation of the vortex velocity from the vorticity equations of motion, an ingredient that is lacking from the vortex creep theory of AAPS and its extensions. The activation energy for vortex slippage is obtained from a detailed study of the mechanics and energetics of vortex motion. A key conclusion of this paper is that the “linear creep” regime invoked in vortex creep theory is not realized for physically reasonable parameters. The “linear creep” regime relies on vortex motion anti-parallel to the Magnus force to be nearly equal to vortex motion parallel to the Magnus force. Here I show that the anti-parallel motion is so strongly suppressed by the large vortex self-energy as to be negligible. Fits to post-glitch data that invoke this regime (Alpar et al. 1993, 1994, 1996) should therefore be reassessed. Without a “linear

---

<sup>1</sup>In AAPS,  $t_d$  is denoted  $t_o$ , and is called the “offset time”, while  $t_r$  is denoted  $\tau$ , and is called the “relaxation time”.

creep” regime of vortex response, the problem of vortex motion through thermal activation becomes strongly constrained; effectively, only the “non-linear” regime of thermally-activated vortex motion remains. A second important conclusion is that “superweak pinning”, which plays a key role in vortex creep theory, probably does not occur but is eliminated by thermal fluctuations.

The other conclusions of this paper are in *qualitative* agreement with the “non-linear” regime studied by AAPS. In particular:

1. If pinning occurs, post-glitch response through thermally-activated vortex slippage consists of two distinct phases. First, the pinned superfluid is *decoupled* from the crust over a timescale  $t_d$ , during which the external torque acts on a lower moment of inertia, and the crust spins down at a greater rate. After a time  $t_d$ , a region in which there is pinning will recouple over a timescale  $t_r$ . The total recovery time from the glitch is  $t_d + t_r$ . Post-glitch response generally depends *non-linearly* on the initial conditions.
2. For a glitch in the spin rate of magnitude  $\Delta\nu$ , the decoupling time is

$$t_d \simeq 7 \left( \frac{t_{sd}}{10^4 \text{ yr}} \right) \left( \frac{\Delta\nu/\nu}{10^{-6}} \right) \text{ days}, \quad (1)$$

where  $t_{sd}$  is the spin-down age. This timescale represents a *lower limit* for the duration of post-glitch response.

3. If the recoupling time  $t_r$  satisfies  $t_r < t_d$ , as can happen in a large glitch, and a portion  $\Delta I_s$  of the core’s moment of inertia participates in the response, the fractional change in  $\dot{\nu}$  is

$$\frac{\delta\dot{\nu}}{|\dot{\nu}|} = -\frac{\Delta I_s}{I} \frac{1}{1 + (e^{t_d/t_r} - 1)e^{-t/t_r}}, \quad (2)$$

depicted by the dashed curve in Figure 9. Identification of this characteristic non-exponential response through analyses of existing and future timing data would give evidence that thermally-activated vortex slippage plays a key role in post-glitch response.

4. If a glitch is small enough that  $t_d \ll t_r$  is satisfied, the glitch recovers as  $e^{-t/t_r}$ .

Post-glitch response in the vortex slippage theory of this paper is mathematically identical to the “non-linear creep” regime of AAPS, but with crucial quantitative differences. In this paper, the scaling of the recoupling time with the pinning energy  $E_p$  is found to be  $t_r \propto E_p^{0.9}$  for the inner crust and  $t_r \propto E_p^{3/5}$  for the outer core. By contrast, AAPS conclude

that  $t_r$  is *independent* of  $E_p$  in the “non-linear” regime, and exponentially dependent on  $E_p$  in the “linear regime”.

To summarize, the vortex theory of AAPS and its extensions has two regimes of vortex motion, the “non-linear” and “linear” regimes, while the vortex slippage theory given here has only one, the “non-linear” regime. The vortex slippage theory presented here predicts a minimum post-glitch response time of  $t_d$ , which is determined by the size of the glitch. Vortex creep theory invokes a “linear creep” regime that is not realized for physically reasonable parameters, and that gives very short recovery times without a waiting time  $t_d$  before the system recouples. By contrast, in the vortex slippage theory developed in this paper, the total post-glitch response time can only exceed  $t_d$ , giving strong constraints on the theory.

This paper presents the theory of thermally-activated vortex slippage, with preliminary comparison with data; detailed comparisons with data and constraints of the theory will be given in a forthcoming publication. In Section 2, the implications of post-glitch response are described in terms of a simple but quite general model of the coupling between the crust and the liquid interior. In Section 3, the response of a neutron star without pinning is reviewed. In Section 4, pinning of vortices to inner-crust nuclei and outer-core flux tubes is described. In Section 5, the theory of thermally-activated vortex slippage is developed. In Section 6, the mechanics and energetics of vortex pinning is discussed. In Section 7, the relaxation dynamics are calculated and described. In Section 8, the coupling timescales are estimated for the inner crust and the outer core. In Section 9, preliminary comparisons of the calculations with observed post-glitch response are made. In Section 10, the results are compared with the previous work of AAPS and its extensions. Appendix A determines the conditions under which vortex pinning disappears, and vortex motion enters the drag regime. Appendix B shows that vortex motion against the Magnus force is strongly suppressed. Appendix C shows that vortex pinning is unlikely to occur in the denser regions of the inner crust, including the pasta region, so that the “superweak pinning” regime proposed by AAPS, a regime that plays a key role in vortex creep theory, is probably ruled out.

## 2. Post-glitch Response: General Considerations

Post-glitch response shows bewildering variety, with no clear systematics (Lyne et al. 2000; Wang et al. 2000). Most glitches are consistent with simple steps in the spin rate, with a recovery fraction  $Q \ll 1$  over timescales of hundreds to thousands of days, as shown schematically in Figure 1. In many pulsars, the Vela pulsar for example, the spin-down rate of the star does not recover to its post-glitch value before the next glitch occurs (Cordes et al. 1988; Lyne et al. 1996; Dodson et al. 2002, 2007), indicating that rotational equilibrium

is never reached; the internal torque on the star never becomes constant. The post-glitch response of such pulsars is problematic to study theoretically, since the glitch cannot be described as a perturbation about a state of rotational equilibrium.

Consider the stellar crust plus charges, component  $C$  of moment of inertia  $I_c$ , coupled to the superfluid interior, component  $S$  of moment of inertia  $I_s$  comprising the neutron superfluids of both the inner crust and the core. Let a glitch occur at  $t = 0$ . To account for the fact that most glitches do not recover completely ( $Q < 1$ ), I introduce a third component, component  $L$ , which imparts angular momentum  $J_l$  at the time of the glitch. Unlike  $C$  and  $S$ , this “loose screw” is never in rotational equilibrium; it couples to  $C$  only at the time of the glitch, but remains otherwise completely decoupled. As described in Section 8, much of the neutron star interior can remain decoupled by glitches if there is pinning; decoupled components in either the crust or the core could represent the loose screw that drives glitches.

Assuming axisymmetry for simplicity, the rotational dynamics of the system is given by

$$I_c \dot{\Omega}_c + \int dI_s \dot{\Omega}_s = N_{\text{ext}} + J_l \delta(t), \quad (3)$$

where  $N_{\text{ext}}$  is the external spin-down torque on  $C$ . Sufficiently long after the glitch, the system will relax to *spin-down equilibrium*, with  $\dot{\Omega}_c = \dot{\Omega}_s = \dot{\Omega}_0$ , where  $\dot{\Omega}_0$  is the equilibrium spin-down rate of both  $C$  and  $S$ . The external torque is given by  $N_{\text{ext}} = I \dot{\Omega}_0$ , where  $I \equiv I_c + I_s$ . (Note that  $I$  excludes component  $L$ ). Defining the *lag*  $\omega(r, t) \equiv \Omega_s(r, t) - \Omega_c(t)$ , where  $r$  is the polar radius, Equation [3] can be rewritten as

$$\dot{\Omega}_c = -\frac{1}{I} \int dI_s \dot{\omega}(r, t) + \dot{\Omega}_0 + \frac{J_l}{I} \delta(t). \quad (4)$$

The change in spin rate across the glitch is

$$\Delta\Omega_c \equiv \Omega_c(0+) - \Omega_c(0-) = -\frac{1}{I} \int dI_s [\omega(r, 0+) - \omega(r, 0-)] + \frac{J_l}{I}, \quad (5)$$

and the solution to Equation [4] for  $t > 0$  is

$$\Omega_c(t) - \Omega_c(0+) = -\frac{1}{I} \int dI_s [\omega(r, t) - \omega(r, 0+)] + \dot{\Omega}_0 t, \quad (6)$$

assuming constant  $N_{\text{ext}}$ . The *spin rate residual* is the difference between the post-glitch spin rate and the value it would have had if the glitch had not occurred:

$$\delta\Omega_c(t) \equiv \Omega_c(t) - [\Omega_c(0-) + \dot{\Omega}_0 t]. \quad (7)$$

Adding Equations [5] and [6], and using the definition of the spin residual, gives

$$\delta\Omega_c(t) = -\frac{1}{I} \int dI_s [\omega(r, t) - \omega(r, 0-)] + \frac{J_l}{I}. \quad (8)$$

Of general interest is coupling between  $C$  and  $S$  that depends only on the local lag  $\omega(r, t)$ :

$$\dot{\Omega}_s(r, t) = f(\omega(r, t)), \quad (9)$$

where the coupling could be linear or non-linear in  $\omega$ . The state of spin-down equilibrium,  $\omega_0(r)$ , is given by the solution to

$$\dot{\Omega}_0 = f(\omega_0(r)). \quad (10)$$

Let  $S$  and  $C$  be in spin-down equilibrium just before the glitch. Then

$$\delta\Omega_c(t) = -\frac{1}{I} \int dI_s [\omega(r, t) - \omega_0(r)] + \frac{J_l}{I}. \quad (11)$$

At late times after the glitch,  $\omega(r, t)$  recovers to  $\omega_0(r)$ , and the residual becomes

$$\lim_{t \rightarrow \infty} \delta\Omega_c(t) = \frac{J_l}{I} = (1 - Q)\Delta\Omega_c. \quad (12)$$

From Equation [3],  $I_c\Delta\Omega_c = J_l$ , so that

$$Q = \frac{I_s}{I}. \quad (13)$$

That many observed glitches have  $Q \ll 1$  with recovery of the spin-down rate to its pre-glitch value suggests, in the context of this simple model, that glitches are driven by an out-of-equilibrium component, and that only a small fraction of the superfluid is associated with post-glitch response.<sup>2</sup>

### 3. Dynamical Response without Vortex Pinning

The dynamics of a superfluid is determined by the motion of the vortices, which is in turn determined by the dissipative forces on the rotating superfluid. In regions of the star where there is no vortex pinning, vortex motion is determined by drag forces. Here I review the dynamics in this regime.

---

<sup>2</sup> More generally, we might expect that some fraction  $f$  of the angular momentum imparted to  $C$  at the time of the glitch comes from  $L$ , with the remainder coming from  $S$ . For this situation,  $Q$  lies in the range

$$\frac{I_s}{I} \leq Q \leq 1. \quad (14)$$

where  $Q = I_s/I$  corresponds to  $f = 1$ , while  $Q = 1$  corresponds to  $f = 0$ . Henceforth I take  $f = 1$ , a restriction that does not affect the conclusions.



Suppose a straight vortex is moving at velocity  $\mathbf{v}_v$  with respect to its environment. The environment could be the nuclear lattice of the inner crust, or the proton-electron fluid of the outer core. The motion of a straight vortex is given by balance between the Magnus force on the vortex and the drag force:

$$\rho_s \boldsymbol{\kappa} \times (\mathbf{v}_v - \mathbf{v}_s) - \eta \mathbf{v}_v = 0, \quad (15)$$

where  $\mathbf{v}_s$  is the flow velocity of the ambient superfluid in the rest frame of the environment,  $\rho_s$  is the superfluid mass density,  $\kappa = h/2m_n$  is the vorticity quantum where  $m_n$  is the neutron mass,  $\boldsymbol{\kappa}$  is directed along the vortex, and  $\eta$  is the drag coefficient.<sup>3</sup> In cylindrical coordinates  $(r, \phi, z)$ , with  $z$  and  $\boldsymbol{\kappa}$  along the rotation axis, the vortex velocity is given by the solution of Equation [15]; see Bildsten & Epstein (1989) and Epstein & Baym (1992):

$$\mathbf{v}_v = v_s \left( \frac{1}{2} \sin 2\theta_d \hat{r} + \cos^2 \theta_d \hat{\phi} \right) = v_s \cos \theta_d \left( \sin \theta_d \hat{r} + \cos \theta_d \hat{\phi} \right) = r\omega \cos \theta_d \hat{n}, \quad (16)$$

where the *dissipation angle*  $\theta_d$  is given by

$$\tan \theta_d \equiv \frac{\eta}{\rho_s \kappa}. \quad (17)$$

The vortex moves in direction  $\hat{n}$ , at an angle  $\theta_d$  with respect to  $\mathbf{v}_s$  with a component away from the rotation axis for positive lag  $\omega$ . An important feature of vortex dynamics is that local forces determine the vortex velocity, not the vortex acceleration.

The dissipation angle is simply related to the relaxation time of the system. Assuming axisymmetry, the angular acceleration of the superfluid follows from vorticity conservation (AAPS; Link et al. 1993)

$$\dot{\Omega}_s(r, t) = -\frac{1}{r} \left( 2\Omega_s(r, t) + r \frac{\partial}{\partial r} \Omega_s(r, t) \right) \mathbf{v}_v \cdot \hat{r}, \quad (18)$$

and is determined by the radial component of the vortex velocity which vanishes in the limit of zero dissipation ( $\theta_d = 0$ ). Assuming uniform superfluid rotation  $\partial\Omega_s/\partial r = 0$  for simplicity, the equation of motion for the angular velocity lag  $\omega \equiv \Omega_s - \Omega_c$  is, from Equation [3],

$$\dot{\omega} = \frac{I}{I_c} (|\dot{\Omega}_0| + \dot{\Omega}_s) - \frac{J_l}{I_c} \delta(t). \quad (19)$$

Linearizing Equation [18], assuming constant  $\theta_d$ , and using Equation [16], gives

$$\dot{\Omega}_s = -\omega \Omega_s \sin 2\theta_d, \quad (20)$$

---

<sup>3</sup> In the low-temperature environment of a neutron star, a vortex has negligible effective mass; its velocity is determined entirely by  $\mathbf{v}_s$  and local forces (Baym & Chandler 1983).

where  $\Omega_s$  is the unperturbed rotational velocity of the superfluid. Assuming spin-down equilibrium with  $\omega(0-) = \omega_0$  just before the glitch, the solution is

$$\omega(t) = \omega_0 + (\omega(0+) - \omega_0)e^{-t/t_r} \quad t_r = \frac{I_c}{I} \frac{1}{\Omega_s \sin 2\theta_d}. \quad (21)$$

From Equation [19], the equilibrium lag is

$$\omega_0 = \frac{I}{I_c} t_r |\dot{\Omega}_0|. \quad (22)$$

In the  $C + S + L$  model of Section 2, with a spin glitch driven by angular momentum from components  $L$ , the response for uniform rotation follows from Equations [11], [12], and [3]:

$$\frac{\delta\Omega_c(t)}{\Delta\Omega_c} = 1 - Q(1 - e^{-t/t_r}) \quad Q = \frac{I_s}{I}. \quad (23)$$

In this linear treatment, the timescale of relaxation is independent of the size of the glitch.

As described below, vortices are expected to pin to nuclei in the inner crust and to flux tubes in the outer core (if the outer core is a type II superconductor). Pinning, though, is not expected to occur everywhere in the star. Let us therefore first consider calculated values for the drag strength without pinning, beginning with the inner crust.

If vortices in the inner crust move in the drag regime, the dominant drag at low lag arises from scattering of the moving vortex against the electron-phonon system of the lattice. Jones (1990) finds  $3 \times 10^{-5} \lesssim \sin 2\theta_d \lesssim 10^{-6}$ , with a typical relaxation time of

$$t_r = 0.2 \frac{I}{I_c} \left( \frac{\nu}{10 \text{ Hz}} \right)^{-1} \left( \frac{\sin 2\theta_d}{10^{-6}} \right)^{-1} \text{ days}, \quad (24)$$

where  $\nu$  is the stellar spin rate. Relaxation through this process is shorter than observed, but the timescale increases significantly as the interaction energy between a nucleus and a vortex is reduced.

Bildsten & Epstein (1989) studied the scattering of electrons with the electron cloud induced around a vortex through its interaction with nuclei. They found  $\sin 2\theta_d \lesssim 10^{-10}$ , corresponding to a relaxation time of 2000 d for  $\nu = 10$  Hz.

Feibelman (1971) considered the scattering of electrons with the magnetic moments of thermally-excited neutrons in the vortex core. The results are strongly sensitive to the neutron pairing gap and to the temperature. From these calculations, using a range of plausible pairing gaps,  $\sin 2\theta_d$  can range from  $\sim 10^{-8}$  to effectively zero.

In the outer core, entrainment of the neutron and proton mass currents when both species are superfluid endows a vortex with a magnetic field of  $B_v \sim 10^{14}$  G (Alpar et al. 1984c). Electron scattering with the strongly-magnetized vortex cores gives  $\sin 2\theta_d \sim 10^{-3}$  (Alpar & Sauls 1988). Hence, if there is no pinning in the core, electron scattering is so effective that the neutral and charged fluids of the core corotate over timescales  $\gtrsim 10^3 \Omega_c^{-1}$ . The core liquid is thus typically considered to corotate with the crust. Sedrakian & Sedrakian (2005) and Sedrakian et al. (1995) have obtained the opposite conclusion; ignoring the natal magnetic field of the neutron star, Sedrakian & Sedrakian (2005) and Sedrakian et al. (1995) argue that magnetic flux tubes of the outer core form clusters around vortices, which could increase the coupling time to observable timescales of days or longer. They suggest that post-glitch response has a core component. The effects of the natal magnetic field on these conclusions have not been studied, and could prove to be important.

The point of view taken in this paper is that post-glitch response could involve both the inner-crust and core superfluids, and both possibilities will be considered.

## 4. Vortex Pinning

### 4.1. Pinning of Vortices to Nuclei in the Inner Crust

As originally pointed out by Pines (1971) and elaborated upon by Anderson & Itoh (1975) and Alpar (1977), vortices of the inner crust interact with nuclei. The main contribution to this interaction is the density dependence of the superfluid condensation energy per particle. When the increase of energy associated with the destruction of superfluidity within the vortex core exceeds the corresponding increase inside the nucleus, the energy cost is minimized if the vortex overlaps with the nucleus, giving an attractive interaction. If the inequality goes the other way, the energy is minimized if the vortices can get as far from nuclei as possible, in which case vortices could pin to the interstices of the nuclear lattice. Pinning is predicted to be strongest in the denser regions of the inner crust. Recent pinning calculations generally agree on the magnitude and density dependence of  $E_p$ , but not its sign. Donati & Pizzochero (2006) find that the vortex-nucleus interaction energy is  $E_p \simeq 3$  MeV, and attractive, for baryon densities  $\rho_b$  in the narrow range  $3 \times 10^{13} < \rho_b < 5 \times 10^{13}$  g cm<sup>-3</sup>. Avogadro et al. (2007) find a similar interaction strength in this density range, though repulsive. Both calculations show a sharp drop in  $|E_p|$  to nearly zero above  $\rho_b \simeq 6 \times 10^{13}$  g cm<sup>-3</sup>. These calculations did not address the spatial dependence of the interaction, and so only estimates of the pinning force based on the relevant length scales could be obtained. The length scale of the interaction is of order the coherence length  $\sim \xi_n$  of the neutron superfluid, and so the force per pinning site is  $F_p \sim E_p/\xi_n$  for pinning to nuclei. This estimate

should apply for a repulsive interaction as well. A vortex is an object with finite rigidity (see below), and in order to move through the lattice it must be brought close to nuclei that repel the vortex over a length scale  $\xi_n$ . Hence, nuclear and interstitial pinning should be very similar.<sup>4</sup> Epstein & Baym (1988), using Ginzburg-Landau theory, obtained  $E_p \simeq 10$  MeV; Ginzburg-Landau theory is however inadequate for this problem, since the superfluid coherence length is comparable to the size of a nucleus.

Above a baryon density  $\rho_b \simeq 6 \times 10^{13}$  g cm<sup>-3</sup>, the pinning situation is unclear. The coherence length exceeds the nuclear spacing (Schwenk et al. 2003; Cao et al. 2006), which weakens pinning. At  $\rho_b \simeq 10^{14}$  g cm<sup>-3</sup>, the nuclei acquire non-spherical pasta shapes (Ravenhall et al. 1983). Pinning to nuclear pasta is probably weaker than pinning to spherical nuclei. Hence, the base of the inner crust could represent a physically distinct region with relatively weak pinning or no pinning. Pinning to nuclear pasta has been studied by Mochizuki & Izuyama (1995) and Mochizuki et al. (1997), who suggest that a vortex can induce nuclear rod formation along its length, becoming self-pinned. Pinning without idealized geometries has not been studied; a first attempt at this problem is given in Appendix C.

If a vortex could bend to intersect nuclei separated by  $a$ , the pinning force per unit length would be

$$f_p = \frac{F_p}{a} \simeq \frac{E_p}{a\xi_n}, \quad (25)$$

typically of order  $10^{17}$  dyn cm<sup>-1</sup> in the inner crust. This force is reduced by the vortex's large self-energy, or *tension*, associated with the kinetic energy of the flow about the vortex (Thomson 1880; Fetter 1967):

$$T_v = \frac{1}{2} \int d^2r \rho_s \left(\frac{\kappa}{r}\right)^2 = \frac{\rho_s \kappa^2}{4\pi} \Lambda \quad \Lambda \equiv \ln \frac{l_v}{\xi_n}, \quad (26)$$

where  $\rho_s$  is the density of free superfluid neutrons. A lower cut-off at the vortex core radius and an upper cut-off at the inter-vortex separation  $l_v$  have been introduced; the logarithmic factor  $\Lambda$  is typically  $\simeq 3$ , as assumed henceforth. Because the vortex is stiff, it cannot bend to intersect every nucleus, but bends over a length scale  $l_p > a$ , as shown in Figure 2.

Throughout much of the inner crust, most of the neutron superfluid is non-dissipatively *entrained* by the nuclei and does not participate in the superfluid flow. Chamel (2005, 2012)

---

<sup>4</sup>For a repulsive interaction, Donati & Pizzochero (2006) estimate the interaction force per site to be  $F_p \sim E_p/a$ , where  $a$  is the nuclear spacing. Since  $a$  is much larger than  $\xi_n$  in regions where they find the interaction to be repulsive, they conclude that interstitial pinning is relatively unimportant, contrary to the argument given here.

finds that  $\sim 90\%$  of the neutron mass is entrained in the denser regions of the inner crust. The effects of entrainment can be treated by taking

$$\rho_s = f_c \rho_n \quad (27)$$

where  $\rho_n$  is the total mass density in neutrons, both bound to nuclei and unbound,  $\rho_s$  is the density of superfluid *conduction neutrons* that are not entrained by nuclei, and  $f_c \sim 0.1$  is the fraction of of the neutron fluid comprising superfluid conduction neutrons. Accounting for nuclear entrainment, the typical vortex self energy is

$$T_v \simeq 0.6 f_c \rho_{n,14} \text{ MeV fm}^{-1}, \quad (28)$$

where  $\rho_{n,14}$  is the total superfluid mass density in units of  $10^{14} \text{ g cm}^{-3}$ . Tension makes the vortex difficult to bend over the typical nuclear spacing  $a \simeq 50 \text{ fm}$  of the inner crust.

Dynamical simulations of a vortex in a random potential at zero temperature by Link (2009), accounting for vortex tension, show that pinning is inevitable below a critical value of the superfluid flow speed with respect to the lattice, but that the pinning force per unit length  $f_p$  is reduced by a factor  $a/l_p$ , where  $l_p$  is the characteristic bending length of a vortex, typically  $10 - 30a$  (if nuclear entrainment is neglected). A variational estimate (Link 2012b; see also Link & Cutler 2002) gives for the pinning force per unit length

$$f_p = \frac{F_p}{l_p} \simeq \frac{E_p}{a\xi_n} \left( \frac{2E_p}{3aT_v} \right)^{1/2} \quad \text{where} \quad \frac{l_p}{a} = \left( \frac{3aT_v}{2E_p} \right)^{1/2}, \quad (29)$$

typically of order  $10^{16} \text{ dyn cm}^{-1}$ . A similar number was obtained by Grill & Pizzochero (2012).

The critical velocity difference  $v_s$  in the rest frame of the solid above which pinning becomes unstable follows by equating the Magnus force per unit length to the pinning force per unit length. In terms of the critical lag  $\omega_{\text{crit}} = v_{s,\text{crit}}/r$  at polar radius  $r$ , accounting for entrainment by nuclei, the Magnus force is

$$f_c \rho_n \kappa r \omega_{\text{crit}} = f_p. \quad (30)$$

Combining with Equations [28] and [29] gives

$$\omega_{\text{crit}} = \frac{E_p}{r f_c \rho_s \kappa \xi_n l_p} \sim 4 \rho_{n,14}^{-3/2} E_p (\text{MeV})^{3/2} \left( \frac{f_c}{0.1} \right)^{-3/2} \left( \frac{\xi_n}{10 \text{ fm}} \right)^{-1} \left( \frac{r}{10 \text{ km}} \right)^{-1} \text{ rad s}^{-1}. \quad (31)$$

Note that entrainment of the neutron superfluid by nuclei increases  $\omega_{\text{crit}}$  by reducing both the tension and the Magnus force.

For small  $E_p$ , thermal motion of the vortex precludes pinning. As shown in Appendix A, pinning disappears for

$$E_p < 0.04 \text{ MeV} \left( \frac{kT}{10 \text{ keV}} \right)^{3/2} \left( \frac{a}{50 \text{ fm}} \right) \left( \frac{\rho_{n,14}}{0.5} \right)^{1/3} \left( \frac{f_c}{0.1} \right)^{1/3}. \quad (32)$$

Without entrainment, pinning vanishes for  $E_p \lesssim 0.1 \text{ MeV}$ .

As discussed in Appendix C, pinning to nuclei is likely to disappear above a baryon density of  $\rho_b \simeq 6 \times 10^{13}$ . Above this density, the coherence length  $\xi_n$  quickly begins to exceed the size of the Wigner-Seitz cell (Schwenk et al. 2003; Cao et al. 2006), and vortices interact primarily with spatial variations in the number density of nuclei. The effective pinning energy becomes so low that thermal fluctuations preclude pinning unless the interaction energy per nucleus  $E_p$  exceeds  $\simeq 0.4 \text{ MeV}$ . Recent pinning calculations show a sharp drop in  $E_p$  to nearly zero above  $\rho_b \simeq 6 \times 10^{13} \text{ g cm}^{-3}$  (Donati & Pizzochero 2006; Avogadro et al. 2007). These effects appear to eliminate “superweak pinning” proposed by AAPS to exist in this density regime; typical values of  $E_p$  for “superweak pinning” used in vortex creep theory are  $\simeq 0.3 \text{ MeV}$  (*e.g.*, Alpar et al. 1989). For  $\rho_b \gtrsim 6 \times 10^{13} \text{ g cm}^{-3}$  in the inner crust, pinning probably does not occur at all, and vortex motion enters the drag regime.

## 4.2. Pinning of Vortices to Flux Tubes in the Outer Core

The protons of the outer core are predicted to form a type II superconductor. As the protons condensed when the star was young, the very high electrical conductivity of the relativistically-degenerate electrons prevented Meissner expulsion of the core’s natal magnetic field (Baym et al. 1969), and the field formed a dense tangle of magnetic flux tubes with which vortices interact. This primarily magnetic interaction pins the vortices to the magnetic tangle which is frozen to the superconducting fluid. The flux tube tangle will be treated as completely immobile under the stresses exerted by the vortex array.

Overlap of a vortex line and a flux tube is energetically favored because the volume of uncondensed fluid is minimized by such overlap; the interaction energy is  $\sim 0.1 \text{ MeV}$  per junction (Srinivasan et al. 1990). A far larger contribution to the interaction energy is the magnetic interaction between the two structures. The magnetic field in a flux tube is  $B_\Phi \sim 10^{15} \text{ G}$  (Alpar et al. 1984c). The magnetic interaction energy between a vortex and a flux tube  $E_p$  is of order  $B_v B_\Phi V$ , where  $V$  is the overlap volume, and has been estimated to be  $\sim 100 \text{ MeV}$  by a number of authors (Jones 1991; Mendell 1991; Chau et al. 1992; Ruderman et al. 1998; Link 2012a). The angle-averaged interaction energy for the intersection of a

vortex with a flux tube is (Link 2012a)

$$E_p \simeq 10^2 \left( \frac{m_p^*/m_p}{0.5} \right)^{-1/2} \left( \frac{|\delta m_p^*/m_p}{0.5} \right) \left( \frac{x_p}{0.05} \right)^{1/2} \left( \frac{\rho_{n,14}}{4} \right)^{1/2} \text{ MeV}, \quad (33)$$

where  $m_p$  is the bare proton mass,  $m_p^* \equiv m_p + \delta m_p^* \sim m_p/2$  (Sjöberg 1976; Chamel & Haensel 2006) is its effective mass, and  $x_p \simeq 0.05$  is the proton mass fraction. The range of the interaction between a vortex and flux tubes is of order the characteristic radius of a flux tube, or the London length, given by (Alpar et al. 1984c),

$$\Lambda_* = 50 \left( \frac{m_p^*/m_p}{0.5} \right)^{1/2} \left( \frac{x_p}{0.05} \right)^{-1/2} \left( \frac{\rho_{n,14}}{4} \right)^{-1/2} \text{ fm}. \quad (34)$$

The pinning force is  $F_p \sim E_p/\Lambda_*$ , about  $1 \text{ MeV fm}^{-1}$ . For a single vortex immersed in a tangle of flux tubes, the average length between intersections will equal the average distance between flux tubes (Link 2012a),

$$l_p \sim l_\Phi \simeq 5 \times 10^3 B_{12}^{-1/2} \text{ fm}, \quad (35)$$

where  $B_{12}$  is the magnetic field in units of  $10^{12} \text{ G}$ . Note that the relevant field is the average *internal* field of the star, which can be significantly larger than the dipolar component (Braithwaite 2009). Because a vortex must cross a “fence” of flux tubes in order to move, the pinning spacing is not increased by the vortex self energy, as is the case for pinning to nuclei in the inner crust.

In the outer core, entrainment between the protons and neutrons, though essential for pinning, has only a small effect on the free neutron density (Chamel & Haensel 2006; Link 2012a);  $f_c$  is effectively unity in evaluating both the tension and the Magnus force. The critical angular velocity difference  $\omega_{\text{crit}}$  between the neutron superfluid and charged component to which the flux tubes are frozen, is given by

$$\rho_n \kappa r \omega_{\text{crit}} l_\Phi = \frac{E_p}{\Lambda_*}, \quad (36)$$

giving (Link 2012a)

$$\omega_{\text{crit}} \sim 10^{-1} \left( \frac{x_p}{0.05} \right) \frac{|\delta m_p^*|}{m_p^*} \left( \frac{E_p}{100 \text{ MeV}} \right) \left( \frac{r}{10 \text{ km}} \right)^{-1} B_{12}^{1/2} \text{ rad s}^{-1}. \quad (37)$$

As shown in Appendix A, thermal motion eliminates pinning when

$$E_p < 0.3 \text{ MeV} \left( \frac{kT}{10 \text{ keV}} \right)^{3/2} B_{12}^{-1/2}. \quad (38)$$

The large value of  $E_p$  of Equation [33] suggests that pinning occurs wherever type II protons coexist with superfluid neutrons.

### 4.3. Dissipation with Vortex Pinning

Pinning causes differential rotation between superfluid and the crust to develop as the crust is spun down by external torque. If a vortex segment unpins, it will be dragged through its environment at relatively high velocity, and the dissipation will be generally stronger than the processes discussed in Section 3 for small velocities. In the inner crust, pinning of vortices to nuclei sustains velocity differences of  $\sim r\omega_{\text{crit}} \sim 10^6 \text{ cm s}^{-1}$ . The dominant contribution to vortex drag on an unpinned segment is the excitation of Kelvin phonons on the vortex (Epstein & Baym 1992; Jones 1992), giving  $\sin 2\theta_d$  as large as  $\sim 0.1$ . For  $\omega \lesssim 10^{-2} \text{ rad s}^{-1}$ , Kelvin phonon production is expected to be greatly reduced (Jones 1992), with a corresponding reduction in the drag. The reduction has not been calculated.

In the outer core, pinning of vortices to flux tubes produces velocity differences of  $\sim r\omega_{\text{crit}} \sim 10^5 \text{ cm s}^{-1}$ . The strength of vortex drag has not been calculated in this regime, but it is reasonable to expect the dissipation to be stronger than the low velocity limit considered by Alpar et al. (1984c), for which  $\sin 2\theta_d \sim 10^{-3}$ . The motion of vortex segments with respect to flux tubes will also excite Kelvin phonons on the vortices, and produce wave excitations on flux tubes; both processes will contribute to the dissipation, and have not been calculated. Dissipation due to the forcing of vortices through flux tubes at supercritical velocities has been studied by Link (2003).

In the estimates below,  $\sin 2\theta_d > 10^{-2}$  will be assumed for the inner crust, and  $\sin 2\theta_d > 10^{-3}$  will be assumed for the outer core. The coupling timescales calculated in Section 8 depend very weakly on these choices.

## 5. Thermally-activated Vortex Slippage

As a result of vortex pinning to nuclei in the inner crust, and to flux tubes in the outer core, the lag  $\omega$  approaches its local critical value as the charged component is spun down by the electromagnetic torque. Before  $\omega_{\text{crit}}$  is reached, though, vortices will slip over their pinning barriers through thermal activation. I now calculate the vortex slippage velocity.

The superfluid circulation speed around a vortex is inversely proportional to the distance from the vortex. The ratio of the pinning interaction length to the pinning spacing is  $\sim 0.2$  in the inner crust, and  $\sim 0.1$  in the outer core. A pinned vortex will henceforth be treated as a thin string with tension in classical continuum mechanics.

Consider pinning of a vortex along axis  $P_1$ ; see Figure 3. Vortex motion occurs as follows. First, thermal fluctuations excite a vortex segment of length  $L_p$  to a saddle-point



configuration at  $S$  that lies out of the range  $r_0$  of the pinning potential. The saddle-point configuration is shown in Figure 4 for an idealized geometry of a linear array of pinning centers spaced by  $l_p$ . The saddle-point configuration will be described in detail below. In this unstable configuration, the stress on the endpoints of the segment is increased by a factor  $L_p/l_p$ , typically greater than unity. The segment will then “unzip” under the Magnus force until the vortex can reach another prospective pinning axis a distance  $d$  away;  $d = a$  for the inner crust and  $l_\Phi$  for the outer core. During this stage, the vortex segment is out of range of the pinning potential, and drifts at velocity  $\mathbf{v}_v$  in direction  $\hat{n}$ , given by Equation [16], toward axis  $P_2$ . For pinning at  $P_2$  to occur, the vortex segment must unzip to length  $L_f > L_p$ , so that pinning to one site along  $P_2$  is stable. This configuration is shown in Figure 5. The condition for mechanical equilibrium is

$$2T_v \sin \left[ \tan^{-1} \left( \frac{2d}{L_f} \right) \right] \hat{n} - \mathbf{f}_{\text{mag}} L_f = \mathbf{F}_p. \quad (39)$$

Typically  $d \ll L_f$ . Using the same cylindrical coordinate system of Section 3, projecting onto  $\hat{r}$  and  $\hat{\phi}$ , gives

$$\frac{4d}{L_f} T_v \sin \theta_d - f_{\text{mag}} L_f = F_{p,r} \quad \text{and} \quad \frac{4d}{L_f} T_v \cos \theta_d = F_{p,\phi}. \quad (40)$$

Typically we are interested in  $\theta_d \ll 1$ . Noting that  $F_{p,\phi}$  is limited by  $F_p = R_p/r_0$ , gives

$$L_f = \frac{4T_v d r_0}{E_p}. \quad (41)$$

As  $E_p$  is lowered,  $L_f$  typically exceeds  $N_p$ , and the vortex must unzip from many pinning bonds to reach static equilibrium at  $P_2$ .

Meanwhile, the same processes are occurring elsewhere along the portions of the vortex that are still pinned along the initial pinning axis  $P_1$ . The vortex slowly migrates, or *slips*, at angle  $\theta_d$  with respect to  $\mathbf{v}_s$ , but at a speed  $v_v \ll v_s$ . As shown in Appendix B, competing transitions against  $\mathbf{f}_{\text{mag}}$  to states such as  $P'$  are prevented by the strong vortex tension unless the dissipation angle is unexpectedly small. In the inner crust,  $\sin 2\theta_d \gtrsim 10^{-2}$  is expected. With nuclear entrainment ( $f_c = 0.1$ ) and  $E_p = 0.04$  MeV, the lower limit for pinning, the suppression factor is  $e^{-1.5} \simeq 0.22$ , with much greater suppression at higher  $E_p$ . Transitions to  $P'$  become important only for

$$\sin 2\theta_d < 1.5 \times 10^{-4} E_p (\text{MeV})^{-1/2} \left( \frac{f_c \rho_{n,14}}{0.5} \right)^{-1/2} \left( \frac{a}{50 \text{ fm}} \right)^{-1/2} \left( \frac{kT}{10 \text{ keV}} \right) \quad (\text{inner crust}) \quad (42)$$

In the outer core, where  $\sin 2\theta_d \gtrsim 10^{-3}$  is expected, transitions to  $P'$  are suppressed relative to transitions to  $P_2$  by a typical factor  $e^{-5 \times 10^4}$ , independent of  $E_p$ . Transitions to  $P'$  become important only for

$$\sin 2\theta_d < 2 \times 10^{-8} \left( \frac{\rho_{n,14}}{4} \right)^{-1} \left( \frac{kT}{10 \text{ keV}} \right) B_{12}^{1/2} \quad (\text{outer core}). \quad (43)$$

Transitions against  $\mathbf{f}_{\text{mag}}$  can thus be ignored in both the inner crust and the outer core.

The vortex slippage process can be described in terms of a two-state system; 1) the vortex is pinned, with zero velocity and zero energy, or, 2) the vortex is unpinned, moving under drag at velocity  $\mathbf{v}_v$ , with energy  $A$  upon unpinning. The energy  $A$  is the activation energy for unpinning, specified below. The partition function for this two-state system is

$$Z = 1 + e^{-\beta A}. \quad (44)$$

Here  $\beta \equiv (kT)^{-1}$  where  $T$  is the temperature and  $k$  is Boltzmann's constant. For slow vortex slippage,  $e^{-\beta A} \ll 1$  and  $Z \simeq 1$ . The slippage velocity of a typical vortex is given by the statistical average

$$\langle \mathbf{v}_v \rangle_\beta = Z^{-1} e^{-\beta A} \mathbf{v}_v \simeq r\omega \left( \frac{1}{2} \sin 2\theta_d \hat{r} + \cos^2 \theta_d \hat{\phi} \right) e^{-\beta A}. \quad (45)$$

The terms that depend on  $\theta_d$  refer to the forces exerted on the unpinned vortex segment by the environment. In the inner crust, the main dissipative force arises from the excitation of Kelvin waves as a vortex segment moves past nuclei. In the outer core, dissipation arises from electron scattering, but there will also be a contribution from the interaction of the translating segment with flux tubes; see Section 4.3.

This treatment of vortex motion assumes the existence of a well-defined pinned state, which requires  $A \gg kT$ . The limit of no pinning given by Equation [16] is recovered by taking  $A \rightarrow 0$  and  $Z \rightarrow 1$ , the latter replacement corresponding to the vortex having only one state of motion in this limit.

We are interested in the flow dynamics of the system over length scales that exceed the inter-vortex spacing:

$$l_v = \left( \frac{\kappa}{2\Omega_s} \right)^{1/2} = 3 \times 10^{-3} \left( \frac{\Omega_s}{100 \text{ rad s}^{-1}} \right)^{1/2} \text{ cm}. \quad (46)$$

We obtain the desired limit by averaging the slippage velocity of Equation [45] for a single vortex over a bundle of  $N \gg 1$  vortices. Consider a bundle of vortices enclosed by a contour

that spans an area  $S$  that satisfies  $\sqrt{S} \gg l_v$ , and average the vortex slippage velocity over the bundle as follows:

$$\langle \mathbf{v} \rangle = \frac{1}{S} \int dS \langle \mathbf{v} \rangle_\beta. \quad (47)$$

$S$  can be chosen so that it contains many vortices ( $\sqrt{S} \gg l_v$ ), while being small enough that  $A$ ,  $\theta_d$ , and  $\omega$ , which vary over macroscopic scales, are nearly constant. This choice gives the same result as the velocity for a typical vortex (Equation 45):

$$\langle \mathbf{v} \rangle = r\omega \left( \frac{1}{2} \sin 2\theta_d \hat{r} + \cos^2 \theta_d \hat{\phi} \right) e^{-\beta A}, \quad (48)$$

Note that  $\langle \dots \rangle$  denotes both a statistical average and a spatial average. All vortices in the bundle move in the same way on average, so that  $\theta_d$  after spatial averaging takes the same value that appears in Equation [45] for a single vortex. The spatial averaging is similar to the macroscopic averaging procedure introduced by Baym & Chandler (1983).

The equation of motion of the superfluid follows by replacing  $\mathbf{v}_v$  in Equation [18] with  $\langle \mathbf{v}_v \rangle$ :

$$\dot{\Omega}_s(r, t) = -\frac{1}{r} \left( 2\Omega_s(r, t) + r \frac{\partial}{\partial r} \Omega_s(r, t) \right) \langle \mathbf{v}_v \rangle \cdot \hat{r}. \quad (49)$$

As an aside, I now connect the treatment so far to that of introducing a *mutual friction* force into the fluid equations, usually taken to have the following form:

$$\mathbf{f}/\rho_s = \mathcal{B}' \boldsymbol{\omega}_s \times (\mathbf{v}_s - \mathbf{v}_b) + \mathcal{B} \hat{\omega}_s \times (\boldsymbol{\omega}_s \times \{\mathbf{v}_s - \mathbf{v}_b\}), \quad (50)$$

where  $\boldsymbol{\omega} \equiv \nabla \times \mathbf{v}_s$  is the vorticity in the inertial frame,  $\mathbf{v}_b$  is the velocity of the background against which vortices are dragged, and  $\mathcal{B}'$  and  $\mathcal{B}$  are the mutual friction coefficients. In terms of the dissipation angle, the mutual friction coefficients are

$$1 - \mathcal{B}' = \cos^2 \theta_d e^{-\beta A} \ll 1 \quad \mathcal{B} = \frac{1}{2} \sin 2\theta_d e^{-\beta A} \ll 1. \quad (51)$$

Vortex pinning is sometimes considered to be equivalent to the limit of high drag (*e.g.*, Sedrakian et al. 1999; Link 2006; Glampedakis et al. 2008; van Hoven & Levin 2008; Glampedakis & Andersson 2009). Assuming that drag is the only force on a vortex, the vortex velocity in Equation [16] goes to zero in the limit  $\eta \rightarrow \infty$ . This description of vortex pinning is inadequate because it ignores the forces exerted on the vortex by the pinning lattice, which can immobilize the vortex even for zero dissipation. As Equation [48] shows, the vortex speed is  $v_v = e^{-\beta A} v_s \ll v_s$  for  $\eta = 0$  ( $\theta_d = 0$ ). Dissipation determines the direction of vortex slippage, and gives  $\mathbf{v}_v$  a component parallel to  $\hat{r}$  for  $\omega > 0$ , and anti-parallel to

$\hat{r}$  for  $\omega < 0$ . For vortex slippage at low dissipation angle, the mutual friction coefficients satisfy

$$\mathcal{B} \ll 1 - \mathcal{B}' \ll 1, \quad (52)$$

whereas many treatments of vortex pinning assume (*e.g.*, Sedrakian et al. 1999; Link 2006; Glampedakis et al. 2008; van Hoven & Levin 2008; Glampedakis & Andersson 2009)

$$1 - \mathcal{B}' \ll \mathcal{B} \ll 1. \quad (53)$$

This condition implicitly assumes very high drag, and is overly restrictive.

## 6. Mechanics and Energetics of Vortex Unpinning

Consider a vortex in stable equilibrium, pinned to a linear array of equally-spaced pinning sites along the  $z$  axis. In the presence of a Magnus force, the vortex unpins by first assuming the unstable, minimum-energy saddle-point configuration depicted in Figure 4. In the saddle-point configuration, a segment of vortex is free of  $N_p$  pinning bonds. The activation energy  $A$  is equal to the energy difference between this state and the fully pinned state, and is determined by the competition between the Magnus force, the pinning force, and the self-energy (or tension) of the vortex.

Let the shape of the vortex be given by the vector  $\mathbf{u}(z)$ . The energy of a vortex segment of length  $L$  is (Link & Epstein 1991)

$$E = \int_L dz \left[ \frac{T_v}{2} \left| \frac{d\mathbf{u}(z)}{dz} \right|^2 + \rho_p V(u) - \rho_s (\boldsymbol{\kappa} \times \mathbf{v}_s) \cdot \mathbf{u}(z) \right]. \quad (54)$$

The first term is the energy cost of bending a vortex with a self-energy per unit length  $T_v$ . The second term is the pinning interaction, where  $\rho_p = l_p^{-1}$  is the number of pinning sites per unit length and  $l_p$  is the average pinning spacing. The third term is the potential energy associated with the constant Magnus force per unit length.

The dependence of the interaction energy on the separation between a vortex segment and a pinning site is unknown, but will increase from zero to a maximum value  $E_p$  over a length scale  $r_0$ . A physically sensible parameterization for the potential is the continuous piecewise function

$$V(u) = E_p \times \begin{cases} \frac{3}{4} \left( \frac{u}{r_0} \right)^2 - \frac{1}{4} \left( \frac{u}{r_0} \right)^3 & 0 \leq u \leq 2r_0 \\ 1 & u > 2r_0, \end{cases} \quad (55)$$

shown in Figure 6. The corresponding force per pinning site has the following parabolic form:

$$F_p(u) = -\frac{dV}{du} = \begin{cases} -F_{\max} \left[ 1 - \left( \frac{u}{r_0} - 1 \right)^2 \right] & 0 \leq u \leq 2r_0 \\ 0 & u > 2r_0, \end{cases} \quad (56)$$

where the maximum force is  $F_{\max} = 3E_p/4r_0$ . The assumed potential corresponds to the second-order series expansion of the interaction force with a maximum of  $F_{\max}$  at  $r_0$ , and so is of general physical relevance. For pinning of vortices to nuclei in the inner crust, the interaction range  $r_0$  is  $\sim \xi_n$ , and the pinning spacing is  $l_p > a$ . For the pinning of vortices to flux tubes in the outer core, the interaction range  $r_0$  is  $\sim \Lambda_*$ , and the pinning spacing is  $l_p \sim l_\Phi$ .

The large vortex self energy plays an important role in determining the mechanics and energetics of the unpinning process, quantified by the dimensionless tension parameter <sup>5</sup>

$$\mathcal{T} \equiv \frac{T_v r_0^2}{E_p l_p}. \quad (57)$$

If vortex tension were negligible, so that  $\mathcal{T}$  is effectively zero, the flexible vortex could unpin one pinning bond at a time to assume a new, stable configuration. Because  $T_v$  is non-zero, though, the vortex must overcome  $N_p > 1$  pinning bonds in an unpinning event;  $N_p$  is determined by  $\mathcal{T}$ . In the inner crust,

$$\mathcal{T} \simeq \frac{T_v \xi_n^2}{E_p l_p} \simeq 0.31 \rho_{n,14} E_p (\text{MeV})^{-1/2} \left( \frac{f_c}{0.1} \right)^{1/2} \left( \frac{\xi_n}{10 \text{ fm}} \right)^2 \left( \frac{a}{50 \text{ fm}} \right)^{-3/2} \quad (\text{inner crust}), \quad (58)$$

while in the outer core,

$$\mathcal{T} \simeq \frac{T_v \Lambda_*^2}{E_p l_\Phi} \simeq 0.12 \left( \frac{\rho_{n,14}}{4} \right) \left( \frac{E_p}{100 \text{ MeV}} \right)^{-1} \left( \frac{\Lambda_*}{50 \text{ fm}} \right)^2 B_{12}^{1/2} \quad (\text{outer core}). \quad (59)$$

Minimization of Equation [54] gives the stable and saddle-point vortex configurations and the associated energies; see Link & Epstein (1991) for details. For a linear array of pinning sites with the potential of Equation [55], the number of broken pinning bonds in the saddle-point configuration is

$$N_p \simeq 3.2 \mathcal{T}^{1/2} (1 - \omega/\omega_{\text{crit}})^{-1/4}, \quad (60)$$

---

<sup>5</sup>In the notation of Link & Epstein (1991),  $\tau = \mathcal{T}$ , the pinning energy is  $U_0 = E_p$ , and the pinning spacing is  $l = l_p$ .

and the activation energy is

$$A \simeq 1.6N_p E_p (1 - \omega/\omega_{\text{crit}})^{3/2} \simeq 5.1E_p \mathcal{T}^{1/2} (1 - \omega/\omega_{\text{crit}})^{5/4} \quad (61)$$

These expressions are valid for  $3/4 \leq \omega/\omega_{\text{crit}} < 1$  and  $N_p \gtrsim 3$ . The latter condition gives  $1 - \omega/\omega_{\text{crit}} < \mathcal{T}^2$ ; for typical parameters of the inner crust and the outer core,  $\omega$  will always be very close to  $\omega_{\text{crit}}$ , so that this condition is satisfied. Hence, in both the inner crust and the outer core  $N_p \gg 1$ , and the vortex is effectively stiff for all pinning energies of interest. Vortex stiffness becomes more important as  $E_p$  is reduced. The important effects of vortex stiffness in determining the activation energy were not considered by AAPS or in subsequent development of vortex creep theory.

To see the basic scaling of  $N_p$  and  $A$  with  $\mathcal{T}^{1/2}$ , note that the energy of a vortex segment bent by amplitude  $u$  is, from Equation [54],

$$E \sim \frac{1}{2} T_v \frac{u^2}{L_p} + \frac{L_p}{l_p} E_p, \quad (62)$$

for zero Magnus force. Extremizing the energy in  $L_p$  gives

$$E \sim \left( \frac{2T_v u^2}{E_p l_p} \right)^{1/2} E_p. \quad (63)$$

If the vortex is to unpin, it must be excited to an amplitude comparable to the range of the pinning potential,  $u \sim r_0$ . Hence,

$$A \sim (2\mathcal{T})^{1/2} E_p \sim N_p E_p, \quad (64)$$

where  $N_p = L_p/l_p$  is the characteristic number of bonds set by vortex tension that must be broken for the vortex to unpin.

## 7. Relaxation Dynamics with Vortex Slippage

Suppose a glitch occurs at  $t = 0$ , through some instability that need not be specified for this perturbative analysis, and let us consider the dynamics in the  $C + S + L$  model of Equation [3]. For axisymmetric rotation, the dynamics is given by

$$I_c \dot{\Omega}_c + \int dI_s \dot{\Omega}_s = -I |\dot{\Omega}_0| + J_l \delta(t), \quad (65)$$

$$\dot{\Omega}_s(r, t) = \left( \Omega_s(r, t) + \frac{r}{2} \frac{\partial \Omega_s(r, t)}{\partial r} \right) \omega(r, t) \sin 2\theta_d e^{-\beta A(\omega(r, t))}, \quad (66)$$

where  $r$  is the cylindrical radius. The response of the crust is determined by integrated dynamics of the superfluid on cylindrical shells of radius  $r$ .

The system can be reduced to a single integral equation with some approximations. The second term in parenthesis in Equation [66] is

$$\frac{r}{2} \frac{\partial \Omega_s(r, t)}{\partial r} \simeq \frac{r}{2} \frac{\partial \omega_{\text{crit}}(r)}{\partial r}, \quad (67)$$

where, from Equations [31] and [37],  $\omega_{\text{crit}} \propto r^{-1}$ . Hence,

$$\frac{r}{2} \frac{\partial \Omega_s(r, t)}{\partial r} \simeq -\frac{1}{2} \omega_{\text{crit}}(r). \quad (68)$$

The critical lag  $\omega_{\text{crit}}$  is always much smaller than  $\Omega_s$ , so the second term in Equation [66] can be neglected, giving

$$\dot{\Omega}_s(r, t) = -\Omega_s(r, t) \omega(r, t) \sin 2\theta_d e^{-\beta A(\omega(r, t))}. \quad (69)$$

Expanding  $A(\omega)$  about  $\omega_0$  in the exponential gives

$$\dot{\Omega}_s(r, t) \simeq \dot{\Omega}_0 e^{b(r)(\omega(r, t) - \omega_0(r))} \quad b(r) \equiv -\beta \left. \frac{\partial A}{\partial \omega} \right|_{\omega_0(r)}. \quad (70)$$

Combining this equation with Equation [65] gives the equation of motion for the lag at each polar radius  $r$ , for  $t > 0$

$$\dot{\omega}(r, t) = |\dot{\Omega}_0| (1 - e^{b(r)(\omega(r, t) - \omega_0(r))}) + \frac{1}{I_c} \int dI_s |\dot{\Omega}_0| (1 - e^{b(r)(\omega(r, t) - \omega_0(r))}). \quad (71)$$

Let us assume that the regions with pinning constitute a small fraction of the star's moment of inertia, so that  $I_s \ll I_c$ . In this limit the spatial integral in the above equation can be neglected. With these approximations, the evolution of the lag is determined entirely by its value locally, and the response of the crust can be calculated by integrating  $\omega(r, t)$  over cylindrical shells. These simplifications were introduced by Alpar et al. (1984a).

Ignoring the spatial integral in Equation [71], the solution is (Alpar et al. 1984a; Link et al. 1993)

$$\dot{\omega}(r, t) = |\dot{\Omega}_0| \left[ 1 - \frac{1}{1 + (e^{t_d(r)/t_r(r)} - 1)e^{-t/t_r(r)}} \right]. \quad (72)$$

where

$$t_d(r) \equiv \frac{\omega_0(r) - \omega(r, 0+)}{|\dot{\Omega}_0|} \quad t_r(r) \equiv \frac{1}{b(r)|\dot{\Omega}_0|} \quad (73)$$

Here  $t_d(r)$  is the *decoupling time* of the shell at radius  $r$  and  $t_r$  is the intrinsic *recoupling time* of the shell. In the limit  $t_d \gg t_r$ , a perturbation in  $\omega$  leaves components  $C$  and  $S$  decoupled

for a time  $\sim t_d$ , before the perturbation is damped over a recoupling time  $t_r$ . In the opposite limit  $t_d \ll t_r$ , a perturbation damps over a time  $t_r$ . This behavior is a consequence of the non-linear dependence of the slippage velocity on the initial value of  $\omega$ . Equation [72] was also obtained by AAPS for the special case of the activation energy having linear dependence on  $\omega$ ; the form given here is more general with the quantity  $b$  given in Equation [70].

As a simplification, let us specify the pre-glitch state by assuming that all transient rotational dynamics has damped before the glitch, so that the system is in *spin-down equilibrium* at  $t = 0$ , such that  $\dot{\omega} = 0$ ,  $\dot{\Omega}_s = \dot{\Omega}_c = \dot{\Omega}_0$  for lag  $\omega_0$ . We will find that the post-glitch recovery time of the inner crust greatly exceeds the average interval between glitches, so rotational equilibrium in the inner crust is not reached between glitches (more on this point in Section 8). By contrast, we will find that the core has ample time to recover rotational equilibrium between glitches.

The equilibrium lag  $\omega_0$  is given by the solution to

$$\dot{\Omega}_0 = -\Omega_s(r) \omega_0(r) \sin 2\theta_d e^{-\beta A(\omega_0(r))}. \quad (74)$$

The residual spin rate of the crust is given by Equation [11]:

$$\delta\Omega_c(t) = -\frac{1}{I} \int dI_s [\omega(r, t) - \omega_0(r)] + \frac{J_l}{I}, \quad (75)$$

To determine the form and timescale of the response, I assume for simplicity that the glitch is driven by component  $L$ , so that

$$\omega(r, 0+) = \omega_0(r) + \Delta\Omega_c. \quad (76)$$

The decoupling time is independent of both  $r$  and the details of pinning:

$$t_d = \frac{\Delta\Omega_c}{|\dot{\Omega}_0|} = 2t_{sd} \frac{\Delta\Omega_c}{\Omega_c}, \quad (77)$$

where  $t_{sd} \equiv \Omega_c/2|\dot{\Omega}_c|$  is the spin-down age. The spin rate residual  $\delta\Omega_c$ , in units of the initial spin jump  $\Delta\Omega_c$ , is

$$\frac{\delta\Omega_c(t)}{\Delta\Omega_c} = 1 - \frac{1}{I} \int dI_s \left[ \frac{t}{t_d} - \int_{0+}^t \frac{dt'}{t_d} \frac{1}{1 + (e^{t_d/t_r(r)} - 1)e^{-t'/t_r(r)}} \right]. \quad (78)$$

At late times, the time integral approaches unity, giving

$$\lim_{t \rightarrow \infty} \frac{\delta\Omega_c(t)}{\Delta\Omega_c} = \frac{I_c}{I} = 1 - Q; \quad (79)$$

the glitch recovers by a fraction  $Q = I_s/I$ .



Now consider the pinning region to be in a spherical shell of constant density  $\rho$  and thickness  $\Delta$ , inner radius  $R$ , and outer radius  $R + \Delta$ . The height of the shell in each hemisphere is  $h(r)$ . The response of the crust is given by

$$\frac{\delta\Omega_c(t)}{\Delta\Omega_c} = 1 - \frac{1}{I} \int_0^{R+\Delta} dr 2\pi\rho h(r)r^3 \left[ \frac{t}{t_d} - \int_{0+}^t \frac{dt'}{t_d} \frac{1}{1 + (e^{t_d/t_r(r)} - 1)e^{-t'/t_r(r)}} \right], \quad (80)$$

where

$$h(r) = \begin{cases} \sqrt{(R + \Delta)^2 - r^2} - \sqrt{R^2 - r^2} & r < R \\ \sqrt{(R + \Delta)^2 - r^2} & r \geq R \end{cases} \quad (81)$$

We will see that  $t_r$  scales as  $\omega_{\text{crit}} \propto r^{-1}$ . Cylindrical shells with smaller radii thus have the longest recoupling times, but they also have smaller moments of inertia  $\propto r^4\Delta$ . The response will be largely determined by the relaxation time in the region  $R < r < R + \Delta$ . Let the characteristic recoupling time there be  $t_r(R)$ . Equation [80] then becomes

$$\begin{aligned} \frac{\delta\Omega_c(t)}{\Delta\Omega_c} &\simeq 1 - \frac{I_s}{I} \left[ \frac{t}{t_d} - \int_{0+}^t \frac{dt'}{t_d} \frac{1}{1 + (e^{t_d/t_r(R)} - 1)e^{-t'/t_r(R)}} \right] = \\ &1 - \frac{I_s}{t_d I} \left[ t + t_r(R) \ln \left( \frac{1 + c(R)}{e^{t/t_r(R)} + c(R)} \right) \right] \quad c(R) \equiv e^{t_d/t_r(R)} - 1. \end{aligned} \quad (82)$$

Figure 7 shows that Equation [82] is a good approximation to Equation [80]. Henceforth I write  $t_r(R) = t_r$ .

Now suppose we add concentric spherical shells, each with superfluid moment of inertia  $I_{s,i}$  and characteristic relaxation time  $t_r(R_i) \equiv t_{r,i}$ . Because of the additive nature of the contributions to the post-glitch recovery within the approximations made so far, the total response of the star is

$$\frac{\delta\Omega_c(t)}{\Delta\Omega_c} \simeq 1 - \frac{1}{t_d I} \sum_i I_{s,i} \left[ t + t_{r,i} \ln \left( \frac{1 + c_i}{e^{t/t_{r,i}} + c_i} \right) \right] \quad c_i \equiv e^{t_d/t_{r,i}} - 1, \quad (83)$$

and

$$Q = \frac{1}{I} \sum_i I_{s,i}. \quad (84)$$

For simplicity I continue to consider the response of a star with a single pinning zone, since the results are easily generalized for multiple pinning zones.

In general, the response of the crust has non-linear dependence on the size of the glitch through the appearance of  $t_d$ , and is referred to as the “non-linear creep regime” by Alpar

et al. (1989). The integral of Equation [82] can be evaluated analytically in two limits. If the glitch is small enough that  $t_d \ll t_r$ , expanding the integrand to first order in  $t_d/t_r$  gives

$$\frac{\delta\Omega_c(t)}{\Delta\Omega_c} = 1 - Q(1 - e^{-t/t_r}) \quad t_d \ll t_r, \quad (85)$$

as for the case for linear frictional coupling (Equation 23), but now with a restriction on the glitch magnitude; the response to the glitch consists of *exponential relaxation* over a timescale  $t_r$ . The residual in the spin-down rate,  $\delta\dot{\Omega}_c(t)$ , is

$$\frac{\delta\dot{\Omega}_c(t)}{|\dot{\Omega}_0|} = -Q \frac{\Delta\Omega_c}{|\dot{\Omega}_0| t_r} e^{-t/t_r}. \quad (86)$$

For a single  $S$  component, the glitch-induced discontinuity in the spin-down rate is

$$\frac{\delta\dot{\Omega}_c(0)}{|\dot{\Omega}_0|} = -\frac{I_s \Delta\Omega_c t_{sd}}{I |\dot{\Omega}_0| t_r}. \quad (87)$$

In the opposite limit of a large glitch, so that  $t_d \gg t_r$ , the integrand of Equation [82] becomes a Fermi function

$$\frac{1}{1 + (e^{t_d/t_r} - 1)e^{-t'/t_r}} \simeq \frac{1}{1 + e^{-(t'-t_d)/t_r}}, \quad (88)$$

and the response of the crust is

$$\frac{\delta\Omega_c(t)}{\Delta\Omega_c} = 1 - Q \left[ \frac{t}{t_d} - \frac{t_r}{t_d} \ln(1 + e^{(t-t_d)/t_r}) \right] \quad t_d \gg t_r, \quad (89)$$

The star recovers through *delayed response*, as shown by the dashed curve in Figure 8. The residual in the spin-down rate is

$$\frac{\delta\dot{\Omega}_c(t)}{|\dot{\Omega}_0|} = -Q \frac{\Delta\Omega_c}{|\dot{\Omega}_0|} \frac{1}{1 + e^{(t-t_d)/t_r}} = -\frac{I_s}{I_c} \frac{1}{1 + e^{(t-t_d)/t_r}} \quad t_d \gg t_r. \quad (90)$$

Right after the glitch, the magnitude of the spin rate has increased by  $|\delta\dot{\Omega}_c|/|\dot{\Omega}_c| = I_s/I_c$ . This constant spin rate excess persists for a time  $t_d$ , followed by relatively quick recovery over a timescale  $t_r$ , as shown by the dashed curve in Figure 9. Examples of the general behavior of  $\delta\Omega_c(t)$  and  $\delta\dot{\Omega}_c(t)$  are shown in Figure 8 and 9. The characteristic relaxation time of the system is  $\tau = t_d + t_r$ . Significant deviations from exponential response occur for  $t_d \gtrsim 3t_r$ , corresponding to  $\tau \gtrsim t_d$ .

The recoupling time  $t_r$  depends on the value of the equilibrium lag  $\omega_0$ . The equilibrium lag is given by the solution to Equations [74] and [61]:

$$1 - \frac{\omega_0}{\omega_{\text{crit}}} = \left[ \frac{kT}{5.1 \mathcal{T}^{1/2} E_p} \ln(2t_{sd} \omega_0 \sin 2\theta_d) \right]^{4/5}, \quad (91)$$

where  $\Omega_s \simeq \Omega_c$  was used. For typical parameters, the right-hand side of Equation [91] is much smaller than unity, so that  $\omega_0 \simeq \omega_{\text{crit}}$ ;  $\omega_0$  can be replaced by  $\omega_{\text{crit}}$  to a very good approximation. Equations [73], [70], and [61] give the recoupling time

$$t_r = 0.22 \frac{I_c}{I} \omega_{\text{crit}} |\dot{\Omega}_0|^{-1} (\mathcal{T}^{1/2} \beta E_p)^{-4/5} [\ln(2t_{sd} \omega_{\text{crit}} \sin 2\theta_d)]^{-1/5}. \quad (92)$$

Note the extremely weak dependence on  $t_{sd}$  and  $\theta_d$ , and linear dependence on  $|\dot{\Omega}_0|^{-1}$ . Unlike  $t_d$ , the recoupling time  $t_r$  does not depend on the conditions after the glitch;  $t_r$  is intrinsic to the system (or part of the system), and does not depend the simple  $C+S+L$  model used to calculate  $t_d$ .

The chief mathematical results of the vortex slippage theory developed in this paper are given by Equations [77], [83], and [92]. I now proceed with numerical estimates.

## 8. Estimates of Post-glitch Recovery Timescales

The decoupling time in regions of star in which there is no vortex motion at the time of the glitch is, from Equation [77],

$$t_d = 7 \left( \frac{t_{sd}}{10^4 \text{ yr}} \right) \left( \frac{\Delta\nu/\nu}{10^{-6}} \right) \text{ days} \quad (93)$$

where  $\nu$  is the spin frequency of the pulsar and  $\Delta\nu$  is the change at the glitch. For large glitches in older stars,  $t_d$  can be very long;  $\Delta\nu/\nu = 3 \times 10^{-6}$  gives  $t_d = 210 \text{ d}$  for  $t_{sd} = 10^5 \text{ yr}$ . In the region or regions of the star in which vortex motion drives the glitch,  $t_d$  can be much longer; see below.

The recoupling time  $t_r$  is determined by the pinning parameters. For vortex slippage in the inner crust,  $t_r$  follows from Equations [92], [29], [31], and [58]. Taking  $\sin 2\theta_d = 10^{-2}$  for dissipation through Kelvin phonon production (though the exact value is unimportant),  $t_r$  in terms of fiducial values is

$$t_r \simeq 30 \left( \frac{|\dot{\nu}|}{10^{-11} \text{ s}^{-2}} \right)^{-1} \left( \frac{f_c}{0.1} \right)^{-1.7} \left( \frac{\rho_{n,14}}{0.5} \right)^{-1.7} E_p(\text{MeV})^{0.9} \times \left( \frac{kT}{10 \text{ keV}} \right)^{4/5} \quad (94)$$

$$\left( \frac{kT}{10 \text{ keV}} \right)^{4/5} \left( \frac{a}{50 \text{ fm}} \right)^{-0.9} \left( \frac{\xi_n}{10 \text{ fm}} \right)^{-9/5} \left( \frac{R}{10 \text{ km}} \right)^{-1} \text{ yr}.$$

The population of glitching pulsars shows a range in  $\dot{\nu}$  from  $\sim -10^{-15} \text{ s}^{-2}$  to  $\sim -10^{-9} \text{ s}^{-2}$ , giving values of  $t_r$  from  $\sim 10^2 \text{ d}$  to decades. Nuclear entrainment has the important effect of making  $t_r$  very long by reducing the density of free neutrons. The Magnus force (for given

lag) that drives the system’s recovery to rotational equilibrium is correspondingly reduced, so the recovery time is increased.

Recoupling of the core through vortex slippage occurs much more quickly than in the inner crust. Using Equations [35], [37], and [59] in Equation [92], and taking fiducial values for the outer core, gives:

$$t_r \simeq 3 \left( \frac{|\dot{\nu}|}{10^{-11} \text{ s}^{-2}} \right)^{-1} \left( \frac{\rho_{n,14}}{4} \right)^{-7/5} \left( \frac{kT}{10 \text{ keV}} \right)^{4/5} \left( \frac{E_p}{100 \text{ MeV}} \right)^{3/5} \times \left( \frac{\Lambda_*}{50 \text{ fm}} \right)^{-9/5} \left( \frac{R}{10 \text{ km}} \right)^{-1} B_{12}^{3/10} \text{ days.} \quad (95)$$

While the dipole components of the field typically have  $B_{12} = 1$ , it is the internal field that determines the recoupling time. With relatively weak sensitivity to  $E_p$  and  $B$ , this estimate is more robust than for the inner crust. Higher multipoles could plausibly make  $B$  about ten times larger than the surface field (Braithwaite 2009).

For large glitches,  $t_r$  is typically less than  $t_d$ , and so the response will be the delayed response illustrated by the dashed curves of Figures 8 and 9; see the discussion following Equation [90]. If a moment of inertia  $\Delta I_s$  is decoupled by the glitch, post-glitch response of the core consists of a fixed increase in the magnitude of the spin-down rate by a factor  $\Delta I_s/I_c$ , followed by a relatively quick recovery over a timescale  $t_r$ , after time  $t_d$ .

The large vortex self-energy acts to reduce the recoupling time  $t_r$ ; see Equation [92]. Increasing the tension by a factor of 10 over that used in Equation [26] decreases  $t_r$  by a factor of  $\simeq 5$  in the inner crust and  $\simeq 3$  in the outer core. Vortex tension generally increases vortex mobility, giving shorter recoupling times. The decoupling time  $t_d$  is unaffected.

The estimate of  $t_d$  in Equation [93] applies to all parts of the star in which pinned vortices do not move during the glitch. If some portion  $S'$  of the superfluid interior with a moment of inertia  $I'_s$  drives the glitch, and  $I'_s$  is much less than  $I_c$ , the decoupling time of this region could be very long. By angular momentum conservation

$$I_c \Delta \Omega_c + I'_s \Delta \Omega_s = 0, \quad (96)$$

giving a change in lag in this region given by

$$I \Delta \Omega_c + I'_s \Delta \omega = 0, \quad (97)$$

and a decoupling time of this region of

$$t'_d = \frac{|\Delta \omega|}{|\dot{\Omega}_c|} = \frac{I \Delta \Omega_c}{I'_s |\dot{\Omega}_0|} = 2 \left( \frac{I/I'_s}{10^{-2}} \right) \left( \frac{t_{sd}}{10^4 \text{ yr}} \right) \left( \frac{\Delta \nu/\nu}{10^{-6}} \right) \text{ yr} \quad (98)$$

Such a region could serve as the  $L$  component in the simple model of this paper as follows. After the glitch,  $S'$  remains decoupled from  $C$  for a time  $t'_d$ , and stores angular momentum as the star spins down. After a time  $t'_d$ ,  $S'$  recovers to spin-down equilibrium over the recoupling time  $t'_r$  of that region. An instability drives vortex motion in  $S'$ , creating a glitch, and the process repeats itself. Parts of the inner crust with typically very long coupling times, could serve as the  $L$  component.

For all other parts of the star in which there is pinning,  $t_d$  is the same, and is set by the size of the glitch according to Equation [93].

## 9. Comparison with observed post-glitch response

I now give a brief comparison for two pulsars for which post-glitch response has been measured in detail: the Vela and Crab pulsars. Vela has shown post-glitch response times that range between about 0.5 d and about 400 d. The Crab pulsar has shown post-glitch response times that range from about two days to 100 d. Most glitches show multiple timescales; see the ATNF Pulsar Glitch Catalogue (Manchester et al. 2005) and references therein.

### 9.1. Inner-crust slippage

Equation [94] predicts  $t_r \simeq 10^4$  d for the Vela pulsar, with a relatively small addition to the total relaxation of  $t_d \simeq 20$  d for a typical glitch. For the Crab pulsar the predicted recoupling time is  $t_r \simeq 300$  d, with  $t_d \ll t_r$  because the glitches are generally small. It appears that post-glitch response due to vortex slippage in the inner crust is too slow to reconcile with observations in these two pulsars. Note that  $t_r$  decreases by a factor of about 50 if entrainment is negligible for some reason.

### 9.2. Outer-core crust slippage

For the Vela pulsar, the total relaxation time  $t_d + t_r$  from Equations [93] and [95] is not in significant disagreement with observed relaxation times but the predictions for the Crab pulsar are  $\tau < 0.1$  d, far shorter than observed; details will be given in a subsequent publication.

These preliminary comparisons suggest that most (if not all) aspects of post-glitch

response are not due to thermally-activated vortex activation, but arise from a different process. The dominant process in post-glitch response might be vortex drag in regions where there is no pinning.

## 10. Comparison with Earlier Work

The theory developed here differs significantly from the vortex creep theory of AAPS applied to the inner crust (see, also, Alpar et al. 1984b, 1985, 1986, 1988, 1989, 1993, 1994, 1996) and the extensions of the AAPS theory to vortex creep in the outer core (Sidery & Alpar 2009), and gives different predictions. The differences are due to different treatments of the vortex velocity and different forms for the activation energy.

AAPS and Alpar et al. (1984b) adopt the following expression for the radial component of the creep velocity:

$$\langle \mathbf{v}_v \rangle \cdot \hat{r} = v_0 e^{-\beta E_p (1 - \omega/\omega_{\text{crit}})} - v_0 e^{-E_p \beta (1 + \omega/\omega_{\text{crit}})} = 2v_0 e^{-\beta E_p} \sinh \left( \beta E_p \frac{\omega}{\omega_{\text{crit}}} \right); \quad (99)$$

*c.f.*, Equation [48]. The first term accounts for motion away from the rotation axis, and the second term for motion toward the rotation axis. The factor  $v_0$  is a velocity that AAPS refer to as “a typical velocity of microscopic motion of the vortex lines between pinning centers”; a calculation of  $v_0$  is not given, and  $v_0$  is fixed at a constant value of  $10^7$  cm s<sup>-1</sup> for both the inner crust and outer core. The activation energies for outward (+) and inward (-) vortex motion are assumed to be

$$A_{\pm} = E_p (1 \mp \omega/\omega_{\text{crit}}). \quad (100)$$

This form assumes that vortices are moving in a *linear* bias imposed by the average Magnus force; *c.f.*, Equation [61]. Note that vortex tension does not appear in Equations [99] and [100]; each pinned segment of a vortex is treated effectively as a point particle, without coupling of adjacent segments through tension.

The chief conclusions of the vortex creep theory of AAPS and its extensions are these:

1. For relatively large  $E_p$ , spin-down drives the system to an equilibrium lag  $\omega_0 \lesssim \omega_{\text{crit}}$ . The radial component of the creep velocity becomes, in the theory of AAPS:

$$\langle \mathbf{v}_v \rangle \cdot \hat{r} = v_0 e^{-\beta E_p (1 - \omega/\omega_{\text{crit}})} \quad \omega_0 \lesssim \omega_{\text{crit}}. \quad (101)$$

In the nomenclature of Alpar et al. (1989), this limit is the regime of “non-linear creep”. In this regime, AAPS obtain a decoupling time

$$t_d = 2t_{sd} \frac{\Delta\Omega_c}{\Omega_c}, \quad (102)$$

as in Equation [77]. AAPS obtain a relaxation time, for perturbations about spin-down equilibrium, of

$$t_r = \frac{\omega_{\text{crit}} kT}{|\dot{\Omega}_0| E_p} = \frac{kT}{|\dot{\Omega}_0| \rho_s \kappa r \xi_n a} \quad \text{“non-linear creep”}. \quad (103)$$

As in this paper, post-glitch response consists of exponential decay if  $t_r \gg t_d$  and delayed response if  $t_d \gg t_r$ .

An important difference between the results of this paper and those of AAPS is the dependence of the  $t_r$  on  $E_p$ . In the vortex creep theory of AAPS,  $\omega_{\text{crit}} \propto E_p$ , giving a relaxation time that is *independent of*  $E_p$ . Equation [103] from the theory of AAPS gives

$$t_r \simeq 8 (f_c \rho_{n,14})^{-1} \left( \frac{|\dot{\nu}|}{10^{-11} \text{ s}^{-2}} \right)^{-1} \left( \frac{kT}{10 \text{ keV}} \right) \left( \frac{\xi_n}{10 \text{ fm}} \right)^{-1} \left( \frac{a}{50 \text{ fm}} \right)^{-1} \left( \frac{R}{10 \text{ km}} \right)^{-1} \text{ yr}, \quad (104)$$

far longer than observed, especially if nuclear entrainment with  $f_c < 0.1$  is taken into account; nuclear entrainment could increase this timescale to over a century. These timescales are incompatible with observations.

2. In the opposite limit of low equilibrium lag,  $\omega_0 \ll \omega_{\text{crit}}$ , corresponding to relatively small  $E_p$ , Equations [99] and [100] give for the theory of AAPS:

$$\langle \mathbf{v}_v \rangle \cdot \hat{r} = 2\nu_0 \beta E_p e^{-\beta E_p} \frac{\omega}{\omega_{\text{crit}}} \quad \omega_0 \ll \omega_{\text{crit}}. \quad (105)$$

In the nomenclature of Alpar et al. (1989), this limit is the regime of “linear creep”. In this regime, post-glitch response consists of exponential decay over a timescale that *depends exponentially on*  $E_p$ :

$$t_r = \frac{r \omega_{\text{crit}}}{4 \Omega_s \nu_0} (\beta E_p)^{-1} e^{\beta E_p} \quad \text{“linear creep”}, \quad (106)$$

and the decoupling time  $t_d$  is effectively zero. Equation [106] gives much shorter coupling times than Equation [103]; consequently, the regime of “linear creep” was invoked by Alpar et al. (1993, 1994, 1996) to explain observed post-glitch response.

The “linear regime” of Alpar et al. (1989) depends on competition between the two terms in Equation [99] that gives linear dependence on  $\omega$  for  $\omega \ll \omega_{\text{crit}}$ . As shown in Appendix B, though, thermal activation of vortex segments *against* the Magnus force is prevented by the large vortex tension unless  $\sin 2\theta_d$  is orders of magnitude smaller than expected. Hence, the

second term in Equation [99] should not be present, and the “linear regime” introduced by Alpar et al. (1988, 1989) is not physically realized. The analysis of this paper gives, instead,

$$\langle \mathbf{v}_v \rangle \cdot \hat{r} = \frac{1}{2} r \omega \sin 2\theta_d e^{-\beta A(\omega)}, \quad (107)$$

for any lag. The above expression does not have a linear expansion about  $\omega = 0$ .<sup>6</sup>

The “linear creep” regime was invoked to fit glitch data by Alpar et al. (1993, 1994, 1996). In fitting to eight glitches in the Vela pulsar, Alpar et al. (1993) included three linear response terms, that is simple exponentials with no time offsets, with relaxation times of  $\sim 30$  d and  $\sim 3$  d, and also 10 hours for the glitch of December 24, 1988. The three contributions to the linear response are assumed to correspond to regions through which no vortex motion occurred, and the pinning is “superweak”. Under this assumption, the change in lag at the glitch for each region is  $\omega_0 - \omega(0+) = \Delta\Omega_c$ . Assuming corotation of the core, as did Alpar et al. (1993), the decoupling time for each region follows from Equation [73]. The glitch magnitudes were in the range  $1.14 \times 10^{-6} \leq \Delta\Omega_c/\Omega_c \leq 3.06 \times 10^{-6}$ , giving a range of decoupling times  $8 \text{ d} \leq t_d \leq 21 \text{ d}$ , significantly larger than the relaxation times of 3 d and 10 hours. Hence, the glitches were too large to exhibit exponential recovery according to the treatment of this paper.

Whether or not the second term in Equation [99] is retained, the creep velocity of AAPS violates the vortex equations of motion, Equations [16] and [48]; Equation [48] contains a factor of  $\omega$  that multiplies the exponential. AAPS effectively fixed

$$\frac{v_s}{2} \sin 2\theta_d = \frac{r\omega}{2} \sin 2\theta_d = v_0 = 10^7 \text{ cm s}^{-1}, \quad (108)$$

For a critical lag of  $\omega_{\text{crit}} = 4 \text{ rad s}^{-1}$  (Equation 31),  $v_0$  cannot exceed  $2 \times 10^6 \text{ cm s}^{-1}$  for any drag process; Equation [108] corresponds to unphysically large drag. For “non-linear creep” the value of  $v_0$  is not very important, since the assumption of spin-down equilibrium gives a weak, logarithmic dependence on the prefactor in Equation [48]; see Equation [92]. More significant is the choice of AAPS of the activation energy of Equation [100], which gives a recoupling time  $t_r$  that is independent of  $E_p$  in this limit, so that the recoupling time depends only on the fact that there is pinning, and not on the strength of the pinning. Equation [100] used by Alpar et al. (1984a) does not follow from consideration of a realistic pinning potential or the large vortex self energy. These considerations give a dependence of the activation energy on  $(1 - \omega/\omega_{\text{crit}})^{5/4}$  for a parabolic pinning force, giving  $t_r \propto E_p^{9/10}$  for the inner crust and  $t_r \propto E_p^{3/5}$  for the outer core.

---

<sup>6</sup>For  $\omega \ll \omega_{\text{crit}}$ , the activation energy diverges as  $\omega^{-1}$  (Link & Epstein 1991).



As Equation [78] shows, the response of the crust to a glitch generally depends non-linearly on the the magnitude of glitch, through the appearance of  $t_d$ . Exponential decay occurs only in the limit  $t_d \ll t_r$ , as for a small glitch. For large glitches, exponential decay occurs only if  $t_r$  exceeds  $t_d$ . For a large glitch ( $\Delta\nu/\nu = 3 \times 10^{-6}$ ), the decoupling time is  $21 (t_{sd}/10^4 \text{ yr}) \text{ d}$ ; in regions with pinning, *exponential decay can occur only over longer timescales than the decoupling time*.

Sidery & Alpar (2009) studied response of the outer core assuming “linear creep”, a regime that is not realized for physically reasonable parameters (see Appendix B). With Equation [105], Sidery & Alpar (2009) obtained a sub-day relaxation time assuming  $E_p \simeq 0.1 \text{ MeV}$ , much smaller than the estimate of  $100 \text{ MeV}$  discussed in Section 4. From the analysis of Appendix A, pinning does not exist for such a low value of  $E_p$ . For larger values of  $E_p$  in the pinning regime,  $t_r$  can be short (*e.g.*,  $E_p = 1 \text{ MeV}$  gives  $t_r = 3 \text{ hours}$  for Vela), but  $t_d$  will still be approximately one week for  $\Delta\nu/\nu = 10^{-6}$ .

## 11. Conclusions

Two chief conclusions of this paper are:

1. The “linear creep” regime introduced by Alpar et al. (1988, 1989) and invoked in fits to post glitch response (Alpar et al. 1993, 1994, 1996) is not realized for physically reasonable parameters, a conclusion that strongly constrains possible post-glitch response through thermal activation. The validity of fits of vortex creep theory to data, and the conclusions drawn about pinning parameters, should be reassessed.
2. A regime of “superweak pinning”, crucial to the theory of AAPS and its extensions, is probably precluded by thermal fluctuations.

The vortex slippage theory given here has clear, falsifiable predictions:

1. Post-glitch recovery associated with regions in which there is vortex pinning, whether in the inner crust or outer core, requires a time that is *at least* as long as the decoupling time:

$$\text{Recovery time} > t_d \simeq 7 \left( \frac{t_{sd}}{10^4 \text{ yr}} \right) \left( \frac{\Delta\nu/\nu}{10^{-6}} \right) \text{ days.} \quad (109)$$

This timescale is independent of the details of vortex pinning, and so is a robust conclusion within the framework of thermally-activated, post-glitch response.

2. Post-glitch response depends non-linearly on the size of the glitch. For a glitch that is sufficiently large that  $t_d \gg t_r$  is satisfied, the response will consist of *delayed response* over a time  $t_d$ , wherein the star *spins down at a constant, higher rate, before relaxing over a time  $t_r$* . Detection of delayed response over a timescale proportional to the glitch magnitude would represent strong evidence for thermally-activated vortex slippage in neutron stars.
3. Exponential decay can occur only if the glitch is sufficiently small that  $t_d \ll t_r$  is satisfied. Hence, exponential decay can occur only over timescales that exceed  $t_d$ , which is determined by the size of the glitch. Quicker decay is prevented by the non-linear nature of coupling through thermal activation. This conclusion is an important difference between vortex slippage theory and vortex creep theory.
4. Response over a relatively quick timescale  $< t_d$  as has been observed in some pulsars, most notably Vela, cannot be due to thermally-activated vortex motion but must represent a different process, such as drag on vortices in regions where there is no pinning.

Comparison of these predictions with the wealth of glitch data now available will be given in a forthcoming publication, and constraints upon the theory will be obtained.

I am grateful to M. A. Alpar, D. Antonopoulou, N. Chamel, and C. Espinoza for very useful discussions, and to R. I. Epstein for valuable suggestions on the manuscript. I also thank the anonymous referee for very useful criticism. This work was supported by NSF Award AST-1211391 and NASA Award NNX12AF88G.

### A. Transition from Vortex Pinning to Vortex Drag

For a sufficiently weak pinning interaction, the thermal energy per unit length of a vortex will exceed the pinning interaction per unit length. In this limit the concept of pinning is no longer appropriate; vortex motion occurs against a drag force, rather than against pinning barriers. The transition occurs when the pinning energy per unit length  $E_p/l_p$  becomes less than the thermal energy per unit length  $E_T/L$  of a free vortex.

Consider a free vortex in thermal equilibrium with its environment at temperature  $T$ . The equation of motion of the vortex of amplitude  $\mathbf{u}(z, t)$  is (Epstein & Baym 1992)

$$T_v \frac{\partial^2 \mathbf{u}(z, t)}{\partial z^2} + \rho_s \boldsymbol{\kappa} \times \frac{\partial \mathbf{u}(z, t)}{\partial t} = 0. \tag{A1}$$

The solutions at the quantum level are “kelvons”, right and left circularly polarized waves with energies

$$\epsilon_k = \frac{(\hbar k)^2}{2\mu}, \quad (\text{A2})$$

where  $k$  is the wavenumber and  $\mu \equiv \rho_s \kappa \hbar / 2T_v$  is the kelvon effective mass. Typically  $\mu \simeq m_n / 3\pi$  where  $m_n$  is the neutron mass; see Epstein & Baym (1992).

The kelvons behave as a one-dimensional gas of bosons, with two polarization states and zero chemical potential. The thermal energy per unit length is

$$\frac{E_T}{L} = 2 \int_0^\infty \frac{dk}{2\pi} \frac{\epsilon_k}{e^{\beta\epsilon_k} - 1} = 0.52 \frac{\sqrt{\mu}}{\hbar} (kT)^{3/2}. \quad (\text{A3})$$

Evaluating  $l_p$  with Equation [29] for the inner crust gives  $E_p/l_p < E_T/L$  for  $E_p$  in the range

$$E_p < 0.04 \text{ MeV} \left( \frac{kT}{10 \text{ keV}} \right)^{3/2} \left( \frac{a}{50 \text{ fm}} \right) \left( \frac{f_c}{0.1} \right)^{1/3} \left( \frac{\rho_{n,14}}{0.5} \right)^{1/3} \quad (\text{inner crust}). \quad (\text{A4})$$

Using  $l_p$  with Equation [35] for the outer core gives  $E_p/l_p < E_T/L$  for

$$E_p < 0.3 \text{ MeV} \left( \frac{kT}{10 \text{ keV}} \right)^{3/2} B_{12}^{-1/2} \quad (\text{outer core}). \quad (\text{A5})$$

For interaction energies below these upper limits, vortices do not pin.

## B. Vortex Motion Anti-Parallel to the Magnus Force

Equation [48] accounts for thermally-activated motion from pinning location  $P_1$  to  $P_2$ ; see Figure 3. Motion to point  $P'$ , anti-parallel to the Magnus force, is strongly forbidden by vortex tension.

Suppose a segment of vortex of length  $L_p = N_p l_p$  unpins from pinning point  $P_1$ , moves under dissipation at angle  $\theta_d$  with respect to  $\hat{\phi}$ , and repins at a single pinning point  $P_2$  a distance  $d \sin \theta_d$  further from the rotation axis. To reach  $P_2$ , the vortex must unzip to a final length  $L_f = 4T_v dr_0 / E_p$  (Equation 41).

A competing process is for the vortex to go the point  $P'$ , against the Magnus force. After unpinning and unzipping, the vortex can pin at  $P'$  (the condition for mechanical equilibrium is the same as for  $P_2$ ), but must increase its energy through thermal fluctuations by

$$\Delta E = 2f_{\text{mag}} L_f d \sin \theta_d = 8f_c \rho_n \kappa T_v E_p^{-1} d^2 r r_0 \omega \sin \theta_d. \quad (\text{B1})$$

The energy penalty is lowered for low lag and low dissipation, but *increases* with decreasing  $E_p$ , because  $L_f$  becomes larger. Transitions to  $P'$ , by any path, are relevant only if

$$\beta\Delta E \lesssim 1. \quad (\text{B2})$$

To obtain  $\Delta E$ ,  $\omega$  is obtained from the solution

$$\langle \mathbf{v}_v \rangle \cdot \hat{\mathbf{r}} = r\omega \sin 2\theta_d e^{-\beta A} - r\omega \sin 2\theta_d e^{-\beta(A+\Delta E)} = \frac{r}{4t_{sd}}. \quad (\text{B3})$$

The first term accounts for motion to  $P_2$ , while the second term accounts for motion to  $P'$ . Numerical solution to the above equation using the activation energy  $A$  from eq [61], for typical parameters, gives  $\omega_0 \simeq \omega_c$ . The condition  $\beta\Delta E < 1$  gives, for the inner crust, with  $d = a$  and  $t_{sd} = 10^4$  yr,

$$\sin 2\theta_d < 1.5 \times 10^{-4} E_p (\text{MeV})^{-1/2} \left( \frac{f_c \rho_{n,14}}{0.5} \right)^{-1/2} \left( \frac{a}{50 \text{ fm}} \right)^{-1/2} \left( \frac{kT}{10 \text{ keV}} \right) \quad (\text{inner crust}) \quad (\text{B4})$$

Transitions to  $P'$  are important only if  $\sin 2\theta_d$  is smaller than this limit, and are otherwise suppressed by a factor  $e^{-\beta\Delta E}$  relative to transitions to  $P_2$ . In the inner crust,  $\sin 2\theta_d \gtrsim 10^{-2}$  is expected. Consider negligible nuclear entrainment,  $E_p = 0.1$  MeV (the lower limit for pinning),  $kT = 10$  keV,  $\rho_{n,14} = 0.5$ , and  $\sin 2\theta_d \geq 10^{-2}$ . Transitions to  $P'$  are suppressed relative to transitions to  $P_2$  by a typical factor  $\leq e^{-15}$ , with greater suppression for higher  $E_p$ . With nuclear entrainment ( $f_c = 0.1$ ),  $E_p = 0.04$  MeV (the lower limit for pinning),  $\rho_{n,14} = 0.5$ , and  $\sin 2\theta_d \geq 10^{-2}$ , the suppression factor is  $\leq e^{-1.5} \simeq 0.22$ , with greater suppression at higher  $E_p$ .

In the outer core,  $\sin 2\theta_d \gtrsim 10^{-3}$  is expected. Here  $d = l_\Phi$ . Taking  $\rho_{n,14} = 4$ , transitions to  $P'$  are suppressed relative to transitions to  $P_2$  by a typical factor  $\leq e^{-5 \times 10^4}$ , independent of  $E_p$ . The condition  $\beta\Delta E < 1$  is met if

$$\sin 2\theta_d > 2 \times 10^{-8} \left( \frac{\rho_{n,14}}{4} \right)^{-1} \left( \frac{kT}{10 \text{ keV}} \right) B_{12}^{1/2} \quad (\text{outer core}). \quad (\text{B5})$$

Hence, in general, transitions against  $\mathbf{f}_{mag}$  are strongly suppressed by the effects of vortex tension in both the inner crust and the outer core, and are effectively excluded for reasonable values of  $\sin 2\theta_d$ .

### C. Random Pinning

At baryon densities above  $\rho_b \simeq 6.3 \times 10^{13}$  g cm $^{-3}$  in the inner crust, the coherence length  $\xi_n$  begins to exceed the Wigner-Seitz spacing (Schwenk et al. 2003; Cao et al. 2006). A vortex

now encompasses many pinning nuclei, and pinning will be greatly weakened. Alpar et al. (1984a) refer to this regime as “superweak pinning”. A vortex now pins to spatial variations in the number density of pinning potentials; I refer to this regime as “random pinning”. Here I show that random pinning is sufficiently weak that it might be precluded by thermal fluctuations.

Consider a vortex of radius  $\xi_n \gg a$  containing randomly distributed point-like potentials of spacing  $a$  and number density  $n_p = a^{-3}$ . The energy associated with the overlap of the vortex with  $N$  randomly placed potentials of strength  $E_p$  is  $E \simeq N^{1/2} E_p$ . The average interaction energy per potential is  $\langle E_p \rangle = N^{-1/2} E_p$ .

A vortex segment can be regarded as interacting with  $N$  nuclei in a flat disc of radius  $\xi_n$ , thickness  $a$ , and volume  $V = \pi \xi_n^2 a$ , containing  $N = n_p V$  interaction nuclei, giving  $N = n_p \pi \xi_n^2 a$ . A rough estimate of the effective pinning energy per nucleus in this regime is thus

$$\langle E_p \rangle \sim \frac{a}{\sqrt{\pi} \xi_n} E_p. \quad (\text{C1})$$

The effective pinning energy increases as superfluidity weakens, and  $\xi_n$  becomes large.

Chamel (2005, 2012) finds that nuclear entrainment is significant from just above neutron drip to densities somewhat below  $\rho_{b,14} = 1$ , where the effects become relatively small. For random pinning to occur,  $\langle E_p \rangle$  must exceed the lower limit given by [A4] at which thermal excitations preclude pinning, giving

$$E_p > 0.4 \left( \frac{kT}{10 \text{ keV}} \right)^{3/2} \left( \frac{\xi_n}{100 \text{ fm}} \right) \text{ MeV}, \quad (\text{C2})$$

where a value of  $\xi_n$  appropriate to  $\rho_{b,14} = 1$  was used, and  $f_c$  was taken to be unity. Pinning calculations show a sharp drop in  $E_p$  to nearly zero above  $\rho_{b,14} \simeq 0.6$  (Donati & Pizzochero 2006; Avogadro et al. 2007).

These arguments should not be significantly altered in the pasta regime at higher densities. Here  $\xi_n$  is predicted to greatly exceed the cell spacing, and the detailed shapes of the nuclear clusters are unlikely to play an important role in the basic energetics.

These considerations suggest that random or “superweak” pinning probably does not occur at all for  $\rho_b \gtrsim 6 \times 10^{13} \text{ g cm}^{-3}$ , from the denser regions of the inner crust into the pasta region.

## REFERENCES

Alpar, M. A. 1977, *Astrophys. J.*, 213, 527

- Alpar, M. A., Anderson, P. W., Pines, D., & Shaham, J. 1984a, *Astrophys. J.*, 276, 325
- . 1984b, *Astrophys. J.*, 278, 791
- Alpar, M. A., Chau, H. F., Cheng, K. S., & Pines, D. 1993, *Astrophys. J.*, 409, 345
- . 1994, *Astrophys. J.*, 427, L29
- . 1996, *Astrophys. J.*, 459, 706
- Alpar, M. A., Cheng, K. S., & Pines, D. 1989, *Astrophys. J.*, 346, 823
- Alpar, M. A., Cheng, K. S., Pines, D., & Shaham, J. 1988, *Mon. Not. Roy. Astron. Soc.*, 233, 25
- Alpar, M. A., Langer, S. A., & Sauls, J. A. 1984c, *Astrophys. J.*, 282, 533
- Alpar, M. A., Nandkumar, R., & Pines, D. 1985, *Astrophys. J.*, 288, 191
- . 1986, *Astrophys. J.*, 311, 197
- Alpar, M. A. & Sauls, J. A. 1988, *Astrophys. J.*, 327, 723
- Anderson, P. W. & Itoh, N. 1975, *Nature*, 256, 25
- Avogadro, P., Barranco, F., Broglia, R. A., & Vigezzi, E. 2007, *Phys. Rev. C*, 75, 012805
- Baym, G. & Chandler, E. 1983, *J. Low Temp. Phys.*, 50, 57
- Baym, G., Pethick, C., & Pines, D. 1969, *Nature*, 224, 673
- Bildsten, L. & Epstein, R. I. 1989, *Astrophys. J.*, 342, 951
- Braithwaite, J. 2009, *Mon. Not. Roy. Astron. Soc.*, 397, 763
- Cao, L. G., Lombardo, U., & Schuck, P. 2006, *Phys. Rev. C*, 74, 064301
- Chamel, N. 2005, *Nucl. Phys. A*, 747, 109
- . 2012, *Phys. Rev. C*, 85, 035801
- Chamel, N. & Haensel, P. 2006, *Phys. Rev. C*, 73, 045802
- . 2008, *Living Rev. Relativity*, 11, 10
- Chau, H. F., Cheng, K. S., & Ding, K. Y. 1992, *Astrophys. J.*, 399, 213

- Cheng, K. S., Alpar, M. A., Pines, D., & Shaham, J. 1988, *Astrophys. J.*, 330, 835
- Cordes, J. M., Downs, G. S., & Krause-Polstorff, J. 1988, *Astrophys. J.*, 330, 847
- Dean, D. J. & Hjorth-Jensen, M. 2003, *Rev. Mod. Phys.*, 75, 607
- Dodson, R., Lewis, D., & McCulloch, P. 2007, *Astrophys. Space Sci.*, 308, 585
- Dodson, R. G., McCulloch, P. M., & Lewis, D. R. 2002, *Astrophys. J.*, 564, L85
- Donati, P. & Pizzochero, P. M. 2006, *Phys. Lett. B*, 640, 74
- Epstein, R. I. & Baym, G. 1988, *Astrophys. J.*, 328, 680
- . 1992, *Astrophys. J.*, 387, 276
- Espinoza, C. M., Lyne, A. G., Stappers, B. W., & Kramer, M. 2011, *Mon. Not. Roy. Astron. Soc.*, 414, 1679
- Feibelman, P. J. 1971, *Phys. Rev. D*, 4, 1589
- Fetter, A. L. 1967, *Phys. Rev.*, 162, 143
- Ginzburg, V. L. & Kirzhnits, D. A. 1965, *Sov. Phys. JETP*, 20, 1346
- Glampedakis, K. & Andersson, N. 2009, *Phys. Rev. Lett.*, 102, 141101
- Glampedakis, K., Andersson, N., & Jones, D. I. 2008, *Phys. Rev. Lett.*, 100, 081101
- Greenstein, G. 1979, *Astrophys. J.*, 231, 880
- Grill, F. & Pizzochero, P. 2012, *J. Phys., Conf. Ser.*, 342, 012004
- Jones, P. B. 1990, *Mon. Not. Roy. Astron. Soc.*, 243, 257
- . 1991, *Mon. Not. Roy. Astron. Soc.*, 253, 279
- . 1992, *Mon. Not. Roy. Astron. Soc.*, 257, 501
- Link, B. 2003, *Phys. Rev. Lett.*, 91, 101101
- . 2006, *Astron. Astrophys.*, 458, 881
- . 2009, *Phys. Rev. Lett.*, 102, 131101
- . 2012a, *Mon. Not. Roy. Astron. Soc.*, 421, 2682

- . 2012b, *Mon. Not. Roy. Astron. Soc.*, 422, 1640
- Link, B. & Cutler, C. 2002, *Mon. Not. Roy. Astron. Soc.*, 336, 211
- Link, B. & Epstein, R. I. 1991, *Astrophys. J.*, 373, 592
- . 1996, *Astrophys. J.*, 457, 844
- Link, B., Epstein, R. I., & Baym, G. 1993, *Astrophys. J.*, 403, 285
- Lohsen, E. 1975, *Nature*, 258, 688
- Lyne, A. G. 1987, *Nature*, 326, 569
- Lyne, A. G., Pritchard, R. S., Graham-Smith, F., & Camilo, F. 1996, *Nature*, 381, 497
- Lyne, A. G., Shemar, S. L., & Smith, F. G. 2000, *Mon. Not. Roy. Astron. Soc.*, 315, 534
- Manchester, R., Hobbs, G., Teoh, A., & Hobbs, M. 2005, *The Astronomical Journal*, 129, 1993, [www.atnf.csiro.au/research/pulsar/psrcat/](http://www.atnf.csiro.au/research/pulsar/psrcat/)
- Melatos, A., Peralta, C., & Wyithe, S. B. 2008, *Astrophys. J.*, 672, 1103
- Mendell, G. 1991, *Astrophys. J.*, 380, 515
- Migdal, A. B. 1959, *Nucl. Phys.*, 13, 655
- Mochizuki, Y. & Izuyama, T. 1995, *The Astrophysical Journal*, 440, 263
- Mochizuki, Y. S., Oyamatsu, K., & Izuyama, T. 1997, *The Astrophysical Journal*, 489, 848
- Peralta, C. & Melatos, A. 2009, *Astrophys. J.*, 701, L75
- Peralta, C., Melatos, A., Giacobello, M., & Ooi, A. 2006, *Astrophys. J.*, 651, 1079
- Pines, D. 1971, in *Proc. 12th International Conference on Low Temperature Physics*, ed. E. Konda (Tokyo: Kaigaku), 7
- Pizzochero, P. 2011, *Astrophys. J.*, 743, L20
- Ravenhall, D. G., Pethick, C. J., & Wilson, J. R. 1983, *Phys. Rev. Lett.*, 50, 2066
- Ruderman, M. 1991, *Astrophys. J.*, 382, 587
- Ruderman, M., Zhu, T., & Chen, K. 1998, *Astrophys. J.*, 492, 267
- Schwenk, A., Friman, B., & Brown, G. E. 2003, *Nuclear Physics A*, 713, 191



- Sedrakian, A. & Cordes, J. M. 1999, *Mon. Not. Roy. Astron. Soc.*, 307, 365
- Sedrakian, A., Wasserman, I., & Cordes, J. M. 1999, *Astrophys. J.*, 524, 341
- Sedrakian, A. D. & Sedrakian, D. M. 2005, *Astrophys. J.*, 447, 305
- Sedrakian, A. D., Sedrakian, D. M., Cordes, J. M., & Terzian, Y. 1995, *Astrophys. J.*, 447, 324
- Shemar, S. L. & Lyne, A. G. 1996, *Mon. Not. Roy. Astron. Soc.*, 282, 677
- Sidery, T. & Alpar, M. A. 2009, *Mon. Not. Roy. Astron. Soc.*, 400, 1859
- Sjöberg, O. 1976, *Nucl. Phys. A*, 265, 511
- Srinivasan, G., Bhattacharya, D., Muslimov, D., & Tsygan, A. 1990, *Current Sci.*, 59, 31
- Thomson, W. 1880, *Phil. Mag.*, 10, 155
- Tsakadze, J. S. & Tsakadze, S. J. 1980, *J. Low Temp. Phys.*, 39, 649
- van Hoven, M. & Levin, Y. 2008, *Mon. Not. Roy. Astron. Soc.*, 391, 283
- Wang, N., Manchester, R. N., Pace, R. T., Kaspi, V. M., Stappers, B. W., & Lyne, A. G. 2000, *Mon. Not. Roy. Astron. Soc.*, 317, 843
- Wang, N., Wu, K.-J., Manchester, R. N., Zhang, J., Lyne, A. G., & Yusup, A. 2001, *Chinese J. Astron. Astrophys.*, 1, 195

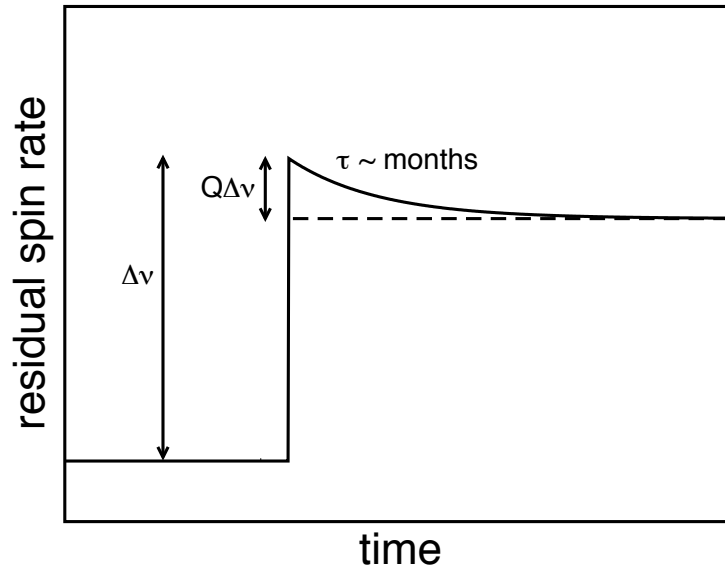


Fig. 1.— Schematic of a typical glitch, showing recovery by a fraction  $Q$ .

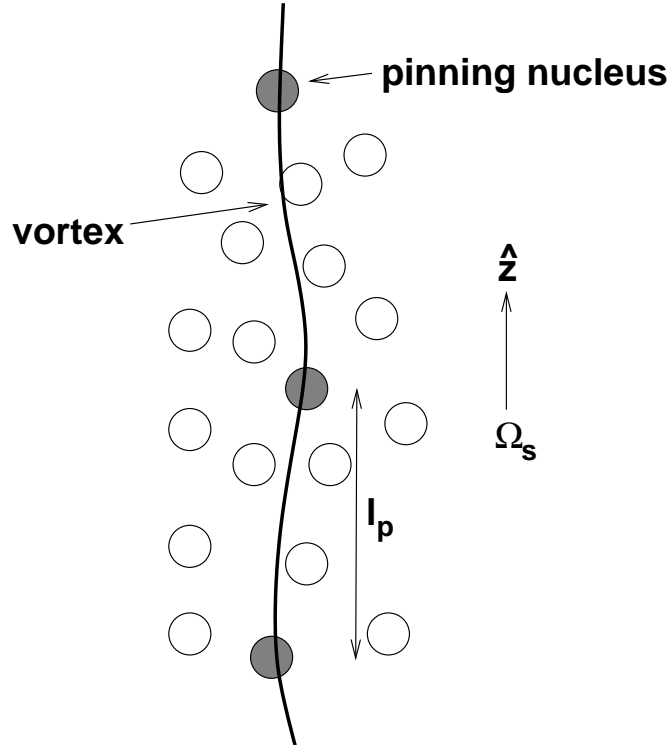


Fig. 2.— Pinning of a vortex to nuclei. The vortex generally follows the rotation axis, but because it has finite rigidity, it cannot bend to intersect every nucleus; rather, the vortex will pin to the shaded “pinning nuclei”, generally missing the unshaded nuclei. The relative importance of the pinning force and the tension force determines the pinning length  $l_p$ . The pinning situation is illustrated here for an amorphous lattice, but these considerations are essentially unaltered for pinning in a regular lattice, since the crystal planes will not generally be aligned with the rotation vector of the superfluid.

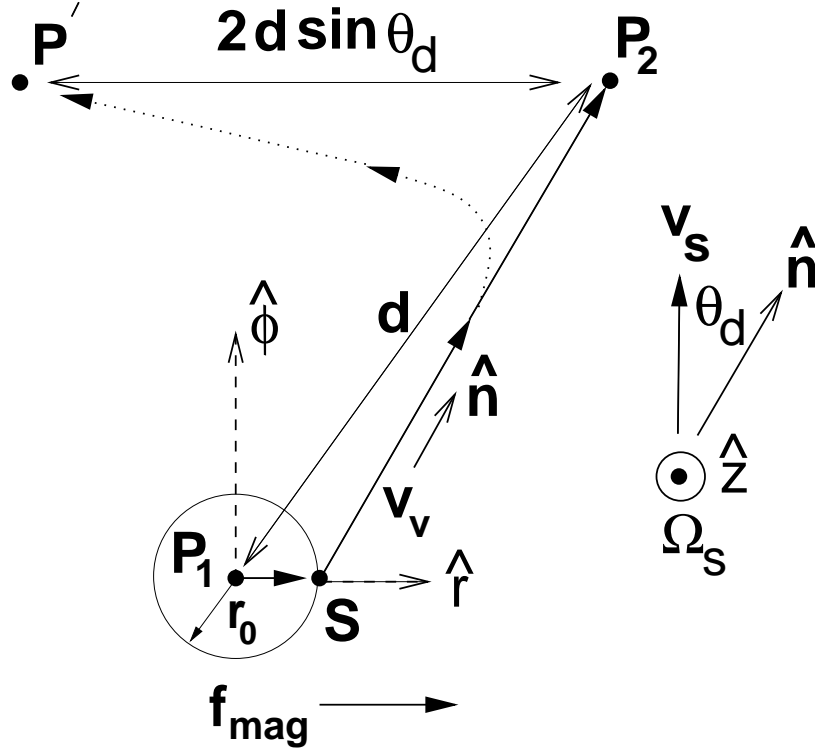


Fig. 3.— Trajectories of vortex segments. The vortex and rotation axes are out of the page. A vortex segment initially pinned along an axis  $P_1$  of pinning sites of spacing  $l_p$  is thermally activated under the Magnus force to saddle-point configuration  $S$ . The segment then translates under dissipation in direction  $\hat{n}$  at velocity  $v_v$  before repinning at a new axis  $P_2$  of pinning sites, a distance  $d$  from  $P_1$ . In this process, the segment moves a distance  $d \sin \theta_d$  away from the rotation axis. Competing processes involving motion  $d \sin \theta_d$  towards the rotation axis, such as to axis  $P'$  along the dotted trajectory, are prevented by the strong vortex self energy; see Appendix B.

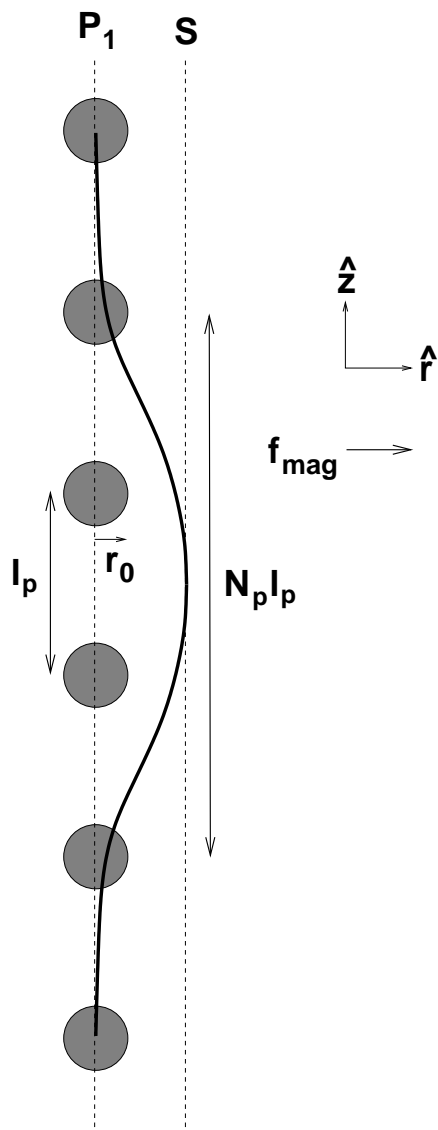


Fig. 4.— Saddle-point configuration in a simplified geometry. A vortex initially pinned along a linear array of pinning sites, nuclei in the inner crust or flux tube intersections in the outer core, is thermally activated to a saddle-point configuration of length  $N_p l_p$  along axis  $S$ . The number of pinning bonds that must break is set by the relative strengths of vortex tension and the pinning energy (through  $\mathcal{T}$ ), and is generally significantly larger than unity. For the inner crust with nuclear spacing  $a$ , the pinning spacing is  $\gtrsim 10a$ , depending on the pinning strength. In the outer core, the pinning spacing is of order the flux tube spacing  $l_\Phi$ .

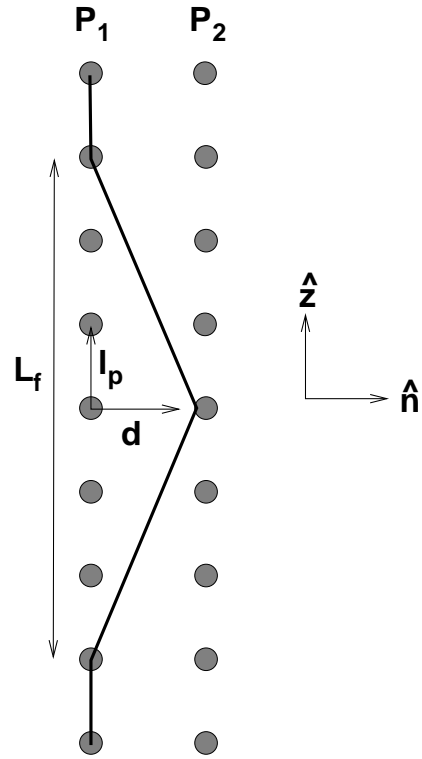


Fig. 5.— New pinned state reached by a vortex segment in a simplified geometry. For the segment to reach a stable configurations as at axis  $P_2$ , it must increase its length to a final length  $L_f$ , greater than the pinning length  $l_p$ , through an “unzipping” process (see text). For the inner crust,  $d$  is approximately the nuclear spacing  $a$ . In the outer core,  $d$  is approximately the flux tube spacing  $l_\Phi$ .

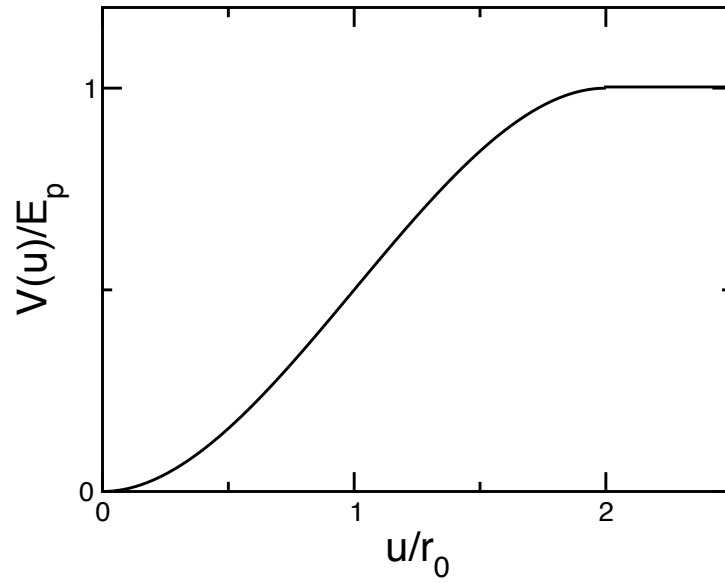


Fig. 6.— Potential of Equation [55], used by Link & Epstein (1991) to obtain the activation energy of Equation [61]. The perpendicular distance of the vortex segment from a pinning site is  $u$ . The maximum force occurs for a displacement  $r_0$ .

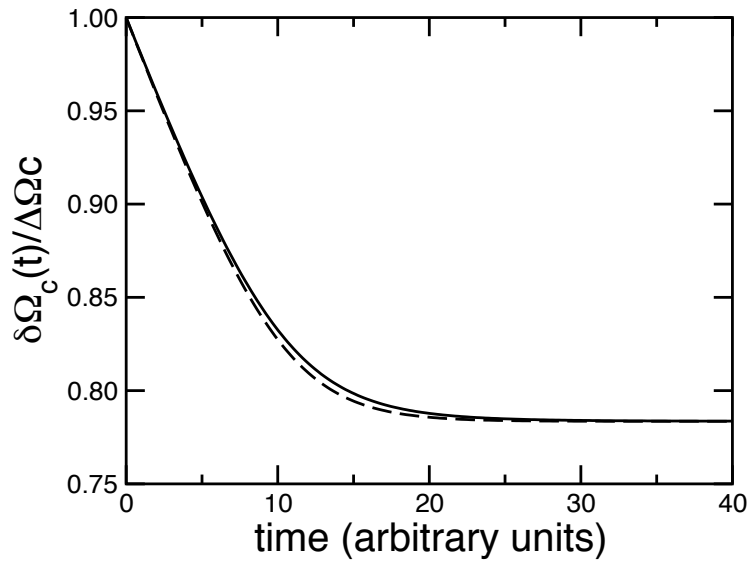


Fig. 7.— Solution given by Equation [80] (solid curve) compared to the simpler solution of Equation [82] (dashed curve), for  $\Delta/R = 0.05$ ,  $I_s/I = 0.22$ ,  $t_d = 10$ , and  $t(R) = 3$ .

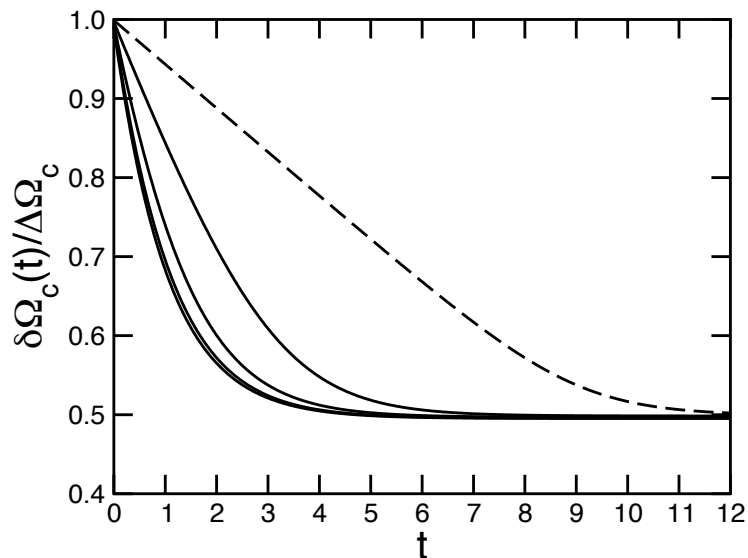


Fig. 8.— Recovery of the crust’s spin rate to a glitch for  $Q = 0.5$ ,  $t_r = 1$ , and (left to right)  $t_d = 0.1, 0.3, 1, 3, 9$ . For  $t_d \gg t_r$ , the response consists of linear decay over a time  $t_d$ , followed by quick recovery to  $1 - Q$  over a timescale  $t_r$ . For  $t_r \gg t_d$ , the response is exponential decay over a timescale  $t_r$ . The total relaxation time is  $\tau = t_d + t_r$ . The dashed curve shows the distinctive signature of recovery of a large glitch through thermal activation of pinned vortices. Significant deviations from exponential response occur for  $t_d \gtrsim 3t_r$ , corresponding to  $\tau \gtrsim t_d$ .



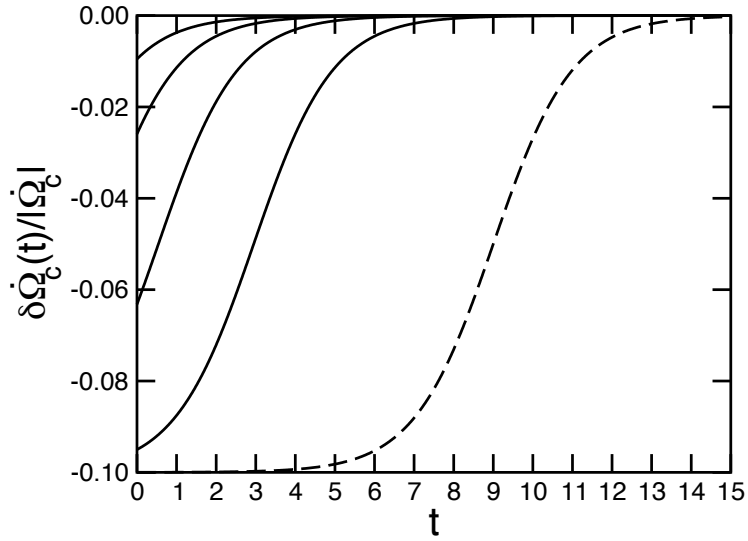


Fig. 9.— Recovery of  $\delta\dot{\Omega}_c$  for  $I_s/I_c = 0.1$ ,  $t_r = 1$ , and (left to right)  $t_d = 0.1, 0.3, 1, 3, 9$ . For  $t_d \gg t_r$ ,  $S$  is decoupled from  $C$  for a time  $t_d$ , giving a fractional decrease of  $-I_s/I_c$  in  $|\delta\dot{\Omega}_c|$ , before rotational equilibrium is restored over a time  $\simeq t_d$ . The dashed curve shows the distinctive signature of recovery of a large glitch through thermal activation of pinned vortices. For  $t_r \gg t_d$ , the recovery consists of exponential decay, with a fractional change in  $\delta\dot{\Omega}_c$  at  $t = 0+$  that is not related to  $I_s/I_c$ . For fixed  $Q$ , the glitch magnitude and  $\delta\dot{\Omega}_c(0+)$  both decrease with  $t_d$  (Equation 77).